available at www.sciencedirect.com

SCIENCE DIRECT®

journal homepage: www.elsevier.com/locate/biochempharm

Gene expression profiles of the rat brain both immediately and 3 months following acute sarin exposure☆

Tirupapuliyur V. Damodaran [a,**], *Anand G. Patel* [a], *Stephen T. Greenfield* [a], *Holly K. Dressman* [b], *Simon M. Lin* [c], *Mohamed B. Abou-Donia* [a,*]

[a] *Department of Pharmacology and Cancer Biology, Duke University Medical Center, Durham, NC 27710, USA*
[b] *Department of Molecular Genetics and Microbiology, Duke University Medical Center, Durham, NC, USA*
[c] *Department Biostatistics and Bioinformatics, Duke University Medical Center, Durham, NC, USA*

ARTICLE INFO

Article history:
Received 6 July 2005
Accepted 10 October 2005

Keywords:
Sarin
Organophosphates
Gene expression
Microarray
Cholinergic system
Acetylcholinesterase

Abbreviations:
ACh, acetylcholine
AChE, acetylcholinesterase
ATP, adenosine tri-phosphate
Bfgf, basic fibroblastic growth factor
BBB, blood brain barrier
CREB, cAMP-response element binding protein
CaM KinaseII, Ca^{2+}/calmodulin-dependent protein kinase II
camp, cyclic AMP
CNS, central nervous system
CRE, cyclic-AMP responsive element
DEPC, diethylpyrocarbonate

ABSTRACT

We have studied sarin-induced global gene expression patterns at an early time point (15 min; $0.5 \times LD_{50}$) and a later time point (3 months; $1 \times LD_{50}$) using Affymetrix: Rat Neurobiology U34 chips in male, Sprague-Dawley rats and have identified a total of 65 (early) and 38 (late) genes showing statistically significant alterations from control levels at 15 min and 3 months, respectively. At the early time point, those that are classified as ion channel, cytoskeletal and cell adhesion molecules, in addition to neuropeptides and their receptors predominated over all other groups. The other groups included: cholinergic signaling, calcium channel and binding proteins, transporters, chemokines, GABAnergic, glutamatergic, aspartate, catecholaminergic, nitric oxide synthase, purinergic, and serotonergic signaling molecules. At the late time point, genes that are classified as calcium channel and binding proteins, cytoskeletal and cell adhesion molecules and GABAnergic signaling molecules were most prominent. Seven molecules (Ania-9, Arrb-1, CX-3C, Gabab-1d, Nos-2a, Nrxn-1b, PDE2) were identified that showed altered persistent expression in both time points. Selected genes from each of these time points were further validated using semi quantitative RT-PCR approaches. Some of the genes that were identified in the present study have been shown to be involved in organophosphate-induced neurotoxicity by both other groups as well as ours. Principal component analysis (PCA) of the expression data from both time points was used for comparative analysis of the gene expression, which indicated that the changes in gene expression were a function of dose and time of euthanasia after the treatment. Our model also predicts that besides dose and duration of post-treatment period, age and possibly other factors may be playing important roles in the regulation of pathways, leading to the neurotoxicity.

☆ Explanations for gene symbols used in the text, figures, and flow charts can be seen in Tables 2 and 3 corresponding to the list of genes and their classifications.

* *Corresponding author*. Tel.: +1 919 684 2221.
** *Co-corresponding author*.
E-mail address: donia@duke.edu (M.B. Abou-Donia).

0006-2952/$ – see front matter © 2005 Elsevier Inc. All rights reserved.
doi:10.1016/j.bcp.2005.10.051

DFP, diisopropylphosphorofluoridate
ERK, extra-cellular signal-regulated kinase
EST, expressed sequence tag
FSH, follicle stimulating hormone
GFAP, glial fibrillary acidic protein
IEG, immediate early gene
JNK, Jun-C N-terminal Kinase
MSK, mitogen and stress activated kinase
mAChE, muscarinic acetylcholine receptor
MAPK, mitogen activated protein kinase
nAChE, nicotinic acetylcholine receptor
NGF, neural growth factor
NF, neurofilament(s)
NO, nitric oxide
OP, organophosphates
OPICN, organophosphorus ester-induced chronic neurotoxicity
OPIDN, organophosphorus ester-induced delayed neurotoxicity
p-CREB, phospho-CREB
PCA, principle component analysis
PCD, programmed cell death
PKA, protein kinase A
RT-PCR, reverse transcriptase-polymerase chain reaction
SAGE, serial analysis of gene expression
SAPK, stress activated protein kinase
SRE, serum response element

1. Introduction

Gene profiling studies have the promise to delineate global alterations in molecular expression as toxic effects, biomarkers, sequence of key events, and mechanisms action of chemicals with multitude of effects, such as sarin (*O*-isopropyl methylphosphonofluoridate) [1]. Sarin was developed during World War II as a nerve agent (nerve agent GB) [2]. Sarin has three distinct neurotoxic actions. First, sarin was tailor-made to irreversibly inhibit acetylcholinesterase (AChE) resulting in the accumulation of acetylcholine (ACh) and subsequent over-stimulation of the nicotinic and muscarinic receptors leading to cholinergic effects and death at high exposure levels [3]. Following sarin release by terrorists at midnight on June 27, 1994, in Matsumoto, Japan, seven persons died and hundreds developed symptoms of cholinergic toxicity [4]. A second terrorist attack by sarin took place in the Tokyo subway at 8:05 a.m. on March 20, 1995, where 5000 individuals were hospitalized and 11 died [5]. Patients with high exposure to sarin exhibited marked muscle fasciculation, tachycardia, high blood pressure (nicotinic responses), sneezing, rhinorrhea, miosis, reduced consciousness, respiratory compromise, seizures, and flaccid paralysis [6].

Another action caused by high exposure to sarin, is a delayed onset of ataxia, accompanied by Wallerian-type degeneration of the axon and myelin of the central and peripheral nervous systems, known as organophosphorus ester-induced delayed neurotoxicity (OPIDN) [7,8]. After exposure to sarin during the Tokyo subway incident, a 51-year-old man who survived the initial acute toxicity, died 15 months later, with neurological deficits and histopathological lesions consistent with OPIDN [9]. This incident demonstrated that humans are more sensitive to OPIDN caused by sarin than the hen, the experimental animal to test for this effect, because it required 26–28 daily doses of sarin LD_{50} (25 μg/kg, i.m.) to produce OPIDN in this species [10].

The third neurotoxic action induced by sarin is a long-term neurological deficits accompanied by brain neuronal cell death that has been characterized recently as organophosphorus ester-induced chronic neurotoxicity (OPICN) [11]. This

effect results from exposure to large toxic or small sub-clinical doses of organophosphates such as sarin. Some victims who exhibited symptoms of acute cholinergic toxicity following the Tokyo subway sarin attack, also developed long-term, chronic neurotoxicity characterized by central nervous deficits and neurobehavioral impairments [12]. Three years after Matsumoto attack, some patients complained of fatigue, shoulder stiffness, weakness, and blurred vision [4]. Early reports indicated that exposure of some individuals to low levels of sarin resulted in persistent neurological and psychiatric abnormalities 5–10 years after exposure [13,14]. In addition, rescue workers and some victims who did not develop any symptoms of acute cholinergic neurotoxicity, nevertheless, exhibited a chronic decline in memory 3 years and 9 months after the Tokyo incident [6]. Also, upon their return from the Persian Gulf War, thousands of American veterans complained from chronic fatigue, muscle and joint pain, ataxia, skin rash, headaches, loss of concentration, forgetfulness, and irritability [15]. Many of the military personnel were exposed to low-level sarin that was released into the atmosphere following the destruction of enemy's chemical arsenal during the war. Animal studies have also demonstrated that exposure to sarin caused brain neuronal cell death [16,17].

Recently, we have carried out several studies on the response of gene expression to organophosphates. A single i.m. dose of $0.5 \times LD_{50}$ sarin resulted in the alteration of the mRNA levels of neuron-specific alpha tubulin [18] and glial fibrillary acidic protein (GFAP) and vimentin [19]. Also, mRNA coding for AChE was differentially elevated [20].

Several methods have been developed to screen cells/tissues for differentially expressed genes, such as differential cDNA library screening [21], subtractive cDNA library screening [22], differential display by PCR [23], and serial analysis of gene expression (SAGE) [24]. While these procedures are suitable for identifying five-fold or greater changes in gene expression (i.e. when genes are either turned off or on), they are inadequate for detecting subtle changes in gene expression. Our Northern and reverse transcriptase polymerize reaction (RT-PCR) results from numerous studies [18,19,25–29] have shown, that the changes in gene expression observed in different organophosphate-treated hen and rat tissues ranged between 30% and 300% of control levels in most situations. On the other hand, high density cDNA arrays allow rapid screening of cells/tissues for gene expression and quantifying changes of 0.5-fold or less with statistically significant levels of accuracy. Recent assessment of the relative impact of the experimental treatment and the platform on measured expression revealed that the biological treatment had a far greater impact on measured expression than did platform for more than 90% of the genes [30].

In this study, we have selected oligonucleotide arrays (Affymetrix) to maximize data output that may reflect all aspects of global gene expression analysis [31]. We also, selected two different doses of sarin, i.e., $0.5 \times LD_{50}$ (sub-lethal) and $1 \times LD_{50}$ (lethal) and the rat neurobiology chips (Affymetrix), containing many key molecules with important functions in the central nervous system (CNS). This report presents the global gene expression data that were used to identify key pathways. Some were triggered immediately, and others showed sustained expression over a period 3 month. These results will help developing a mechanistic view on the possible mode of initiation, modification, persistence or disappearance of distinct molecular lesions that may cause cellular/tissue pathology, leading to clinically and behaviorally observable disorders.

2. Materials and methods

2.1. Materials

A stock solution of sarin (GB, 1.9 mg/ml in saline) was obtained from the U.S. Army Medical Research and Materiel (Command, Fort Dietrich, Frederick, MD, USA). Radioactive [32-P] dATP (3000 Ci/mmol) was purchased from New England Nuclear (Boston, MA, USA). Duralon-UV membranes were purchased from Stratagen (La Jolla, CA, USA) and the Random Primer labeling system was obtained from Invitrogen Life Technologies (Carlsbad, CA, USA). All additional chemicals were purchased from standard sources.

2.2. Animal treatment

2.2.1. Microarray experiment and RT-PCR validation

Young adult male Sprague-Dawley rats, weighing approximately 250 g were purchased from Charles River Labs, Raleigh, NC. Rats were kept in a temperature-controlled room at 21–23 °C with a 12-h light/dark cycle. They were provided with Rat Chow (Purina, St. Louis, MO) and tap water ad libitum. Animal treatment with sarin was carried out in specially designed treatment room at Duke University. All animal treatments and procedures were approved by the Duke University Institutional Animal Care and Use Committee and to conformed to the recommended guidelines of the U.S. Army. For each time point we used the minimum number of animals necessary to produce reliable scientific data. Groups of three rats were treated with a single intra-muscular injection of 50 μg/kg ($0.5 \times LD_{50}$) or 100 μg/kg ($1 \times LD_{50}$) of sarin in normal saline into the thigh muscle. The control group consisting of three rats was injected with 1 ml/kg saline as described above. The rats were examined daily for any clinical signs and weighed two times a week. At the termination of the experiment, the animals were anesthetized with 100 μg/kg of ketamine/xylazine then dissected; the brain was removed and washed thoroughly with ice-cold diethylpyrocarbonate (DEPC)-treated water to remove traces of blood. The rats were sacrificed at 15 min and 3 months post sarin-treatment. Whole brains from both controls and sarin-treated rats were quickly dissected at the end of each time point and snap frozen in liquid nitrogen. Extra care has been taken to preserve the integrity of the whole brain, so that the data we obtain from these animals can be comparable and reliable. The tissues were kept at −70 °C, until used for total RNA extraction.

2.3. Differential expression of CamkII

Other groups of animals were also treated with $0.5 \times LD_{50}$ sarin and were terminated at 24 h after treatment. This study was designed to verify our hypothesis that key genes involved in sarin-induced neurotoxicity might show statistically

significant alterations of mRNA in a total brain RNA approach, in spite of regional variation in gene expression in the brain. Section 2.13 has more details. Appropriate controls were kept for this experiment as mentioned above. At the end of the time point, the animals were euthanized, brain dissected out, and separated into the cortex, cerebellum, midbrain, and brainstem. The tissues were frozen in liquid nitrogen and kept at −70 °C until RNA extraction.

2.4. RNA extraction

Total RNA was extracted using Trizol solution (Invitrogen Life Technology, Carlsbad, CA). The extracted RNA was subjected to several levels of testing before it was declared ready for microarray. The purity and quantity of the RNA was determined by A_{260}/A_{280} ratios and then A_{260}, respectively, using a UV-1601 Shimadzu Spectrophotometer. RNA samples that had good O.D. values (1.8–2.1) were further tested on northern gels for the integrity of both the 28S RNA and 18S RNA by running 5–10 μg of total RNA in denaturing gels and visualizing with ethidium bromide under UV light. If RNA quality came into question at any of these steps, the RNAs were either re-extracted using phenol/chloroform, or purified using a Qiagen RNA cleaning kit until good quality RNA was obtained. In rare instances we repeated the experiment to get good quality RNA.

2.5. Agilent analysis

The RNAs were further subjected to agilent analysis. About 200–250 ng/μl of total RNAs were applied on RNA chip and were analyzed on the Agilent Bioanalyzer 2100. The method involved fractionating the total RNA and observing the integrity on the Bioanalyzer. Minute changes in the integrity of 28S and 18S RNA and other anomalies that might interfere with fluorescent labeling and cRNA synthesis were identified and rectified.

2.6. Chips

Rat Neurobiology U34 array of the Affymetrix gene chip was used, which allowed the monitoring the relative abundance of more than 1200 mRNA transcripts. The sequences that were used to build this array were selected from the UniGene Database. Gene chip probe arrays are made by synthesizing oligonucleotide probes directly onto the glass surface. Each 24 mer oligonucleotide probe is uniquely complementary to a gene, with approximately 16 pairs of oligonucleotide probes used to measure the transcript level of each of the genes represented. This array contains several sequences belonging to rat EST collections. This array also contains several house-keeping genes, and a wide variety of genes representing different cell types, signaling pathways and other functional and structural groups relevant to the nervous system.

2.7. Test chip hybridization

The quality of the RNAs was further determined using the gel image and hybridization of the test chips. These test chips allowed us to optimize the hybridization conditions, besides monitoring the presence of a small subset of characterized genes from various organisms, including mammals, plants and eubacteria. Additionally, the gene chip test 3 array contained a subset of human and mouse housekeeping/maintenance genes shown to be expressed early on fetal development and throughout adulthood. This hybridization also gave clues for predicting the success of chip hybridization experiments.

2.8. Affymetrix chip hybridization

The target chip hybridization followed successful test chip hybridization. All relevant procedures (such as hybridization, washing and data compilation regarding the signal strength of the hybridization) were done at Duke Microarray Center in the Department of Molecular Genetics and Microbiology. The double-stranded cDNA from total RNA (10 μg starting material) was synthesized and isolated from the rat tissues. Biotin-labeled cRNAs was generated by in vitro transcription form the DNA. The cRNAs were fragmented before hybridization, and a hybridization cocktail that included the fragmented cRNAs, probe array controls, bovine serum albumin and herring sperm DNA was prepared. The cRNAs were hybridized to the oligonucleotide probes on the probe arrays for a 16 h incubation at 45 °C. Immediately after the hybridization, the hybridized probe arrays underwent an automated washing and staining protocol on an Affymetrix fluidics station. The DNA chips were scanned with the Affymetrix gene chip scanner and the signals were processed by the gene Chip expression analysis algorithm (v.2; Affymetrix).

2.9. Data analysis

Further data analysis was done using the resources at the Duke University Bioinformatics Shared Resources Consortium. Some of the commonly used programs were used for data analysis included Affymetrix Microarray Software Solutions to identify the list of genes showing statistically significant levels of alteration and the Partek clustering and treeview analysis program to identify clustering of genes that showed alteration, respectively. Identities of the EST clones were verified using the BLAST search program of Duke University Bioinformatics Program.

2.10. Principal component analysis (PCA) of gene expression

(A) Gene Expression Quantification. Rather than using the pre-packaged Affymetrix 5.0 software, Li-Wongfull model [32] was used to quantify the gene expression levels from the hybridization image of Affymetrix chips because it results in fewer false-positive changes.

(B) Data Preprocessing and Empirical Noise Filtering. From the signal processing point of view, the raw expression data should be preprocessed prior to further pattern analysis. It has been suggested that a logarithm transformation not only stabilizes the variation across the expression range, but also is better related to the probe concentration [33]. Thus, the data were log transformed.

The noise in the signal filtered based on the following empirical criteria:

(1) reliable hybridizations, which were indicated by the "detection" in the Affymetrix 5.0 reports, should be present in at least one of the experiment groups;
(2) the "detection" call must be consistent within each experiment groups; and
(3) the CV (as a measurement of variation) within each experiment group should be less than 20%.

(C) Principle component analysis of the experiments. The expression data matrix (rows as experiments, columns as genes) was then analyzed by principle component analysis. The results indicated that the first two components could explain 80% of the variation seen in the data, while the first three components could explain 86% of the variations in the data. Also, the plot gave us a visual representation of the separation of the experimental points.

2.11. *Tree view analysis and clustering*

Hierarchical clustering was applied through the Cluster software program and the results were visualized in Treeview (http://www.microarrays. org/software for computational details). The expression level of each gene relative to the median expression level across all samples was represented by color: red represents expression greater than the mean, and green represents expression less than the mean, and the intensity of each color represents the magnitude of the deviation from the mean.

2.12. *Classification of genes*

The list of genes, obtained after data analysis, was classified as per the description of different classes of molecules playing important but different roles in the nervous system [34].

2.13. *Gene validation*

Two types of validation experiments were used to verify the microarray expression data: (a) Validation by semi-quantitative (relative gene expression) RT-PCR from the total RNA from whole brain that was used to perform the microarray experiments. Several genes were selected based on several hypothetical criteria. We hypothesized that two classes of genes might play key roles in the pathophysiology: (i) genes that persist in two different time points (either up-or down-regulated from its prior altered state or continuing the same trend) should be playing key role in the pathology, repair, and/or other adaptive changes; and (ii) key genes identified to be playing central roles in distinct known pathways of neurotoxicity. (b) Validation by semi-quantitative (relative gene expression) RT-PCR from the total RNA extracted from different regions (such as the cerebrum, cerebellum, brainstem and midbrain) of the CNS with 0.5× LD_{50} sarin treatment was a separate experiment. CamkIIa has been shown to have differential expression patterns in different tissues at distinct time points (1, 5, 10, 20 days post treatment), in an earlier study on the effect of DFP (a structural analogue of sarin) from our group [35]. Its level has been found to be altered at 2 h [36] and also at 3 months (current study) after sarin treatment. Thus, we selected this key gene based on several studies on organophosphate-induced neurotoxicity. The former approach was used to reconfirm the results obtained by microarray, while the latter was used to confirm that the gene expression of selected genes identified by the whole brain approach reflected the gene expression scenario, in spite of expected regional variation.

To accomplish these tasks, the following experiments were carried out:

(A) Gene validation: Semi quantitative RT-PCR approaches [37,38] were used to validate our microarray findings. The relative expression levels of selected genes as compared with the levels of 18S RNA were estimated from the total RNA (originally used to perform the microarray experiments). The linear portion of the PCR amplification (where the density of the PCR product was directly proportional to the amount of template cDNA) for each of the validated genes was determined by serial dilution of the cDNA samples. To relate the expression of the gene of interest to that of the endogenous reference gene, a ratio was determined between the amount of PCR product within the linear amplification range of the target gene and the endogenous reference gene (18S RNA).

(B) Reverse transcription: Using a first strand cDNA synthesis kit (Invitrogen Life Technologies; Carlsbad, CA, USA), 1–2 μg of RNA was reverse transcribed by AMV reverse transcripts. Reverse transcription was primed with random hexamers or oligo-(dt) in a volume of 15 or 33 μl. Polymerase chain reactions were performed with 2–4 μl of the resulting cDNA solution using the following PCR conditions: hot start at 94 C for 4 min, followed by 35 cycles of denaturing at 94 0 C for 60 s, neutralizing to 60 °C for 60 s followed by extension at 72 °C for 1 min. The reactions were also kept at the extension step for one cycle at 72 °C for 7 min. Efforts were taken to ensure that the same set of master mixtures, cDNA stock, and polymerase dilution were always used the relative gene expression experiments. The list of the genes and the primer sets that were used to amplify the gene and product size are given in the Table 1.

(C) Image acquisition and analysis: Following PCR amplifications, 12 μl of PCR product mixed with 2.4 μl of loading solution (40% sucrose, 1 mM EDTA and 0.03% xylene cyanol) was subjected to electrophoresis (100 V dc for 30 min using Horizon® 58, Horizontal Gel Electrophoresis System, Life Technologies, Gaithersburg, MD, USA) in 2% agarose gel under 1× TAE buffer and stained in 0.5 μl g/ml ehidium bromide solution (in 1× TAE) for 30 min. After washing with distilled water, stained gels were placed on a UV transilluminator (302 nm) and photographed with Polaroid-type 667 instant film, which was developed following the manufacturer's suggestion. This high speed photograph was scanned into Photoshop 4.0 (TIFF file) using a UMAX Astra 2400S Scanner. The digital images of the photographs were made at 256 grayscale and a resolution of 400 dpi of the photograph. The bands were quantified using the IP-Lab gel of molecular dynamics. The same rectangular was used to surround the gel bands as well as to surround a blank area of the gel for background

Table 1 – Gene specific primers used in RT-PCR validation experiments

Gene	Forward primer (5′ to 3′)	Reverse primer (5′ to 3′)	Product size (bp)
CX-3C	GGTGGCAAGTTTGAGAAGCGT	GGGCCTTCGGGCCTCCTG	123
PDE2	GCTCTCCAACCAGTTCCTAATC	TCACTTTCTTCGTCTCCACC	260
Nrxn-1b	CACCACATCCACCATTTCC	CACCAACACTGCTTCCTTC	251
Gabbr-1	TGTTCTTGCTGTTGTCTGTC	TCCTTCTTCTCCTCCTTCTTC	291
Ania-9	TCCAACCTTCCTAACAGACC	TCTCACTACAAGTTCTGCTCC	242
CamkIIa	AAGCACCCCAATATCGTCC	TCAGCCTCACTGTAATACTCC	131
Camkd	AAACCAATCCACACTATCATCC	TTCTGCCACTTCCCATCAC	170
IL-10	CTTTCACTTGCCCTCATCC	ACAAACAATACGCCATTCCC	265
Plp	ACTCAGCCAACCTCCCTTAC	ACCTTTAGCATCCCCCAAC	121
Arrb-1	ACCAACAACACCAACAAGAC	ACAATGATACCCAGGATTTCAC	296
Synj1	GCAAGCACAACAAACCAGAA	ACAAACAGGCAGACACCCAC	113
Nos-2	AGACAGAGGCGACAGAAA	GACGAACAGAAATTACATTGGG	159
Nes	ACAAACCTCAACCCTCACC	GCTTCTTTCTCTACCAGTTCCC	122
Map2	ACAGAGAGAGAGAGAGAGAGA	GTCCAGAGTGAAAGCAACC	181
Chrnb4	CGCTCTTCTACACCATCAATC	GTCATCTTCTCCCCACAGTC	100
Chrm2	AACCCAGGATGAAAACACAG	ATGATGAAAGCCAACAGGATAG	287
Actb	CATCCCCCAAAGTTCTAC	CAAAGCCTTCATACATC	213
18S RNA	CATCCCCCAAAGTTCTAC	CAAAGCCTTCATACATC	101

correction. Background values were subtracted from the integrated intensity values of all other data points obtained from the gel bands. Dividing the background corrected value of the candidate genes by the background corrected value of 18S RNA, was normalized the data obtained for each unique gene studied. These background-corrected and normalized values were used for comparison between experimental conditions. Statistical significance was calculated using Student's *t*-test. *P*-value <0.05 was considered significant. The results were presented as percentage values of the controls, where background corrected and normalized control values were used as 100% to calculate the level of alteration for various candidate genes in the treated samples.

(D) DNA sequencing Amplified DNA from the PCR reaction was cloned using a one-shot PCR cloning kit (Invitrogen: Life Technologies; Carlsbad, CA) and the cloned products were sequenced at the Duke University Core Sequencing Facility. Sequence identity was verified using several software programs provided by the Duke University Shared Bioinformatics Program.

3. Results

3.1. Clinical signs

A single intramuscular injection of $1 \times LD_{50}$ sarin in rats caused excessive salivation, severe tremors, seizures, and convulsions, 5–10 min after dosing, followed by a prolonged convulsions lasting about 3 h. One half of this group of animals died within 3 h of dosing, the remaining animals survived the 3-month experiment. Animals treated with $0.5 \times LD_{50}$ did not develop any of the signs cited above, but were inactive, and all of the animals survived the experimental period.

3.2. Early time point (15 min) gene expression profile

A total of 66 genes passed the 0.05 confidence level in the statistical tests. Of these, eight genes were altered in two categories each namely: (a) cytoskeletal and cell adhesion molecules and (b) ion channels. This was followed by the category neuropeptide and their receptors (five genes each). The categories designated as calcium channels and binding proteins and chemokines and their receptors had four genes each. Three genes were identified in each of the categories classified as G-protein coupled receptor and related molecules and purigenic signaling molecules. The following categories had two genes each: (a) cholinergic signaling; (b) energy metabolism; (c) GABAnergic signaling; (d) Glutamergic and aspartate signaling; (e) mitochondria associated proteins (f) myelin proteins; (g) neurotransmission and related transporters; (h) serotonergic signaling; and (i) tyrosine phosphorylation molecules. Additionally, the following groups had one gene in their category: (a) ATPases and ATP-based transporters, (b) catecholaminergic signaling, (c) cyclic nucleotide signaling, (d) cytokines and their receptors, (e) nitric oxide signaling, (f) TNF beta family' and (g) transcription factors (Table 2). The relative levels of gene expression among different genes in the various categories in treated CNS as compared with control levels at the early time point (15 min) are illustrated in Figs. 1–4.

The mRNA percentage levels of alteration for each gene are provided in Table 2. More genes (45) showed up-regulated gene expression (68%) than down-regulation (21) in this time point (32%). Genes that belong to physiologically relevant categories (15 out of 27) such as cholinergic signaling; catecholaminergic signaling; ion channels except one molecule; growth factors; glutamergic and aspartate signaling; GABAergic signaling; chemokines and their receptors; cytokine and their receptors; ATPases and ATP-based transporters; immediate early genes; MAP kinases; nitric oxide signaling; purinergic signaling; transcription factors and TNF beta molecule were up-regulated ranging between $118 \pm 4\%$ and $338 \pm 34\%$. Genes belonging to (4 out of 27) categories such as 'cyclic nucleotide signaling; detoxification molecules; mitochondria associated proteins; and neurotransmission and neurotransmitter transporters showed down-regulation, ranging between $38 \pm 11\%$ and 84% of the control values. The rest of the groups showed both up and down-regulated genes. The highest level of up-

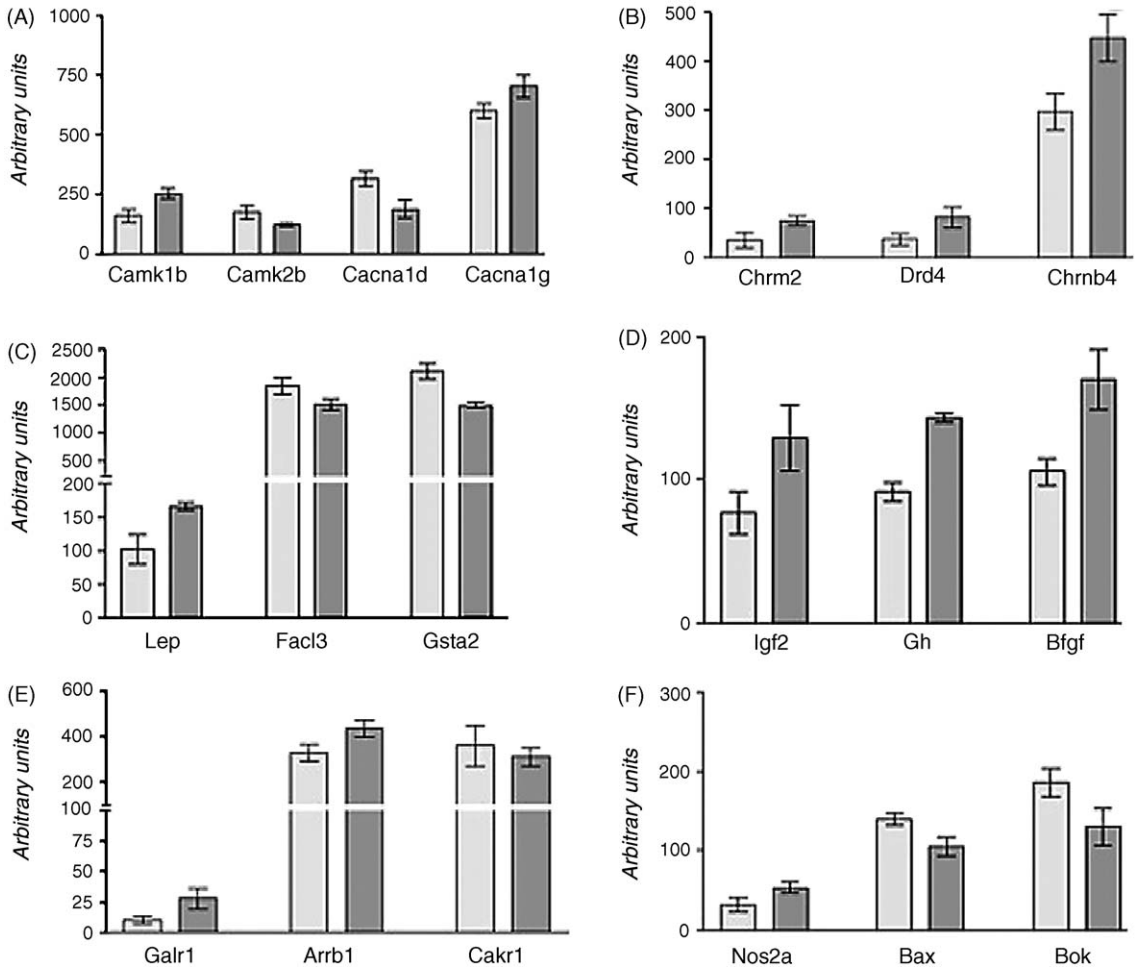

Fig. 1 – Histograms showing the mRNA expression levels at 15 min post-treatment time point for various genes belonging to following categories: (A) calcium channels and binding proteins; (B) cholinergic and catecholaminergic signaling; (C) detoxification and energy metabolism; (D) growth factors; (E) G-protein coupled receptors and inhibitors; (F) mitochondria-associated proteins and nitric oxide signaling. Arbitrary units of fluorescent hybridization data obtained from both control (clear) and treated (shaded) sets for each gene are included in this figure. All data in this figure passed the 0.05 level of statistical significance.

regulation was seen for Ecto-ATPase (334 ± 47%), while the greatest down-regulation was seen for C-kit (23 ± 2%).

3.3. *Genes that were close to 0.05 level significance (but were not included in the list)*

The following genes were considered because of their proximity to the cut-off point and probable relevance to the toxicant-induced physiological changes: (1) rat cytochrome P-450 (65 ± 4%) and (3) NMDA receptor-like long variant (142 ± 2%). The significance of these genes in the pathophysiology is addressed in detail in Section 4.

3.4. *Late time point (3 months) gene expression profile*

A total number of 38 genes reached the required level of significance (0.05 level) of which both calcium channels and binding proteins and immediate early genes had the highest number of genes (four each). These categories were followed by cytoskeletal and cell adhesion molecules and GABAnergic signaling as well as growth factors and inhibitors, each with three genes. Categories that were designated as cyclic nucleotide signaling, cytokines and their receptors; ion channels; and synaptic vesicle proteins and transporters had two genes each in their groups. Other groups such as catecholamine signaling; chemokines; death factors; G-protein coupled receptors; glutamergic and aspartate signaling; metabolism; proteases; Rho-GTPase effector; and tyrosine kinases, each had one gene in their group. Details about the list of these genes are provided in the Table 3. The relative levels of gene expression among different genes of various categories as well as the relative levels between control and treated CNS at 3 months are illustrated in the Figs. 5 and 6.

Unlike the early time point, there were an equal number of genes (19) that showed up-regulation (50%) and down-regulation (50%) at the late time point. In spite of the higher dose of sarin; however, at this time point ($1 \times LD_{50}$), the total number of genes showing statistical significance (0.05 level) was almost half the number at the early time point (with

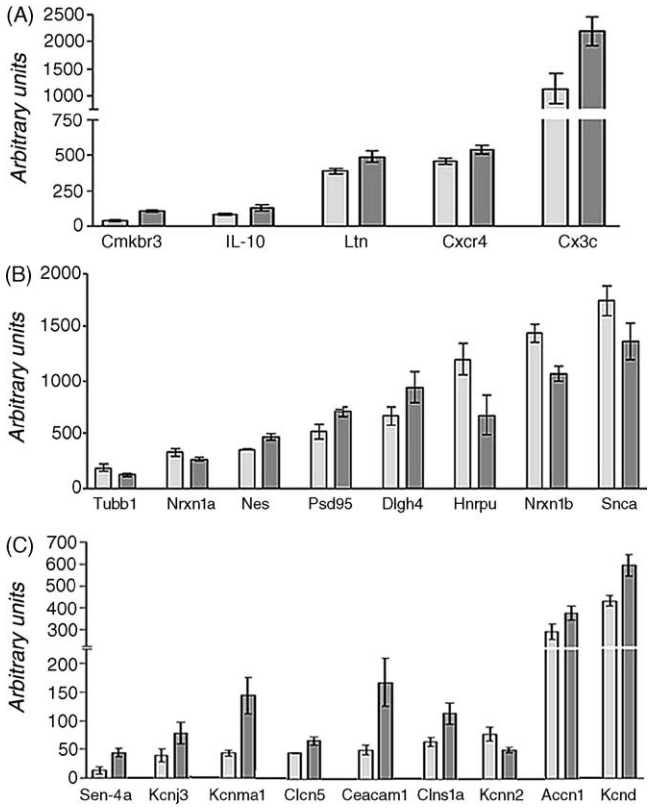

Fig. 2 – Histograms showing the mRNA expression levels at 15 min post-treatment time point for various genes belonging to following categories: (A) cytokines and their receptors; (B) cytoskeletal and cell adhesion molecules; (C) ion channels and ATPases. Arbitrary units of fluorescent hybridization data obtained from both control (clear) and treated (shaded) sets for each gene are included in this figure. All data in this figure passed the 0.05 level of statistical significance.

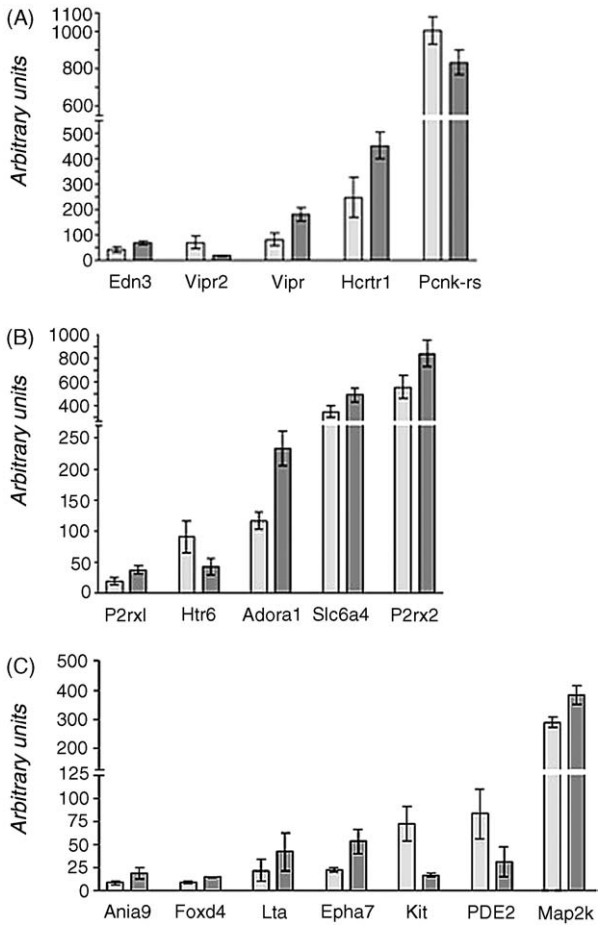

Fig. 3 – Histograms showing the mRNA expression levels at 15 min post-treatment time point for various genes belonging to following categories: (A) neuropeptides and their receptors; (B) purinergic and serotonergic signaling; (C) miscellaneous group containing genes belonging to groups such as IEG (Ania-9), transcription factor (Foxd4), TNF beta family (Lta), tyrosine phosphorylation molecules (Epha7, kit), cyclic nucleotide molecule (PDE2), and kinases (Map2k). Arbitrary units of fluorescent hybridization data obtained from both control (clear) and treated (shaded) sets for each gene are included in this figure. All data in this figure passed the 0.05 level of statistical significance.

$0.5 \times LD_{50}$). Genes belonging to (a) cyclic nucleotide signaling, (b) cytokines and their receptors, (c) G-protein coupled receptor, (d) glutamate receptor all AMPA subtype, GluR1, (e) growth factors and inhibitors, (f) metabolism, and (g) proteases, showed up-regulation. The percentage values of up-regulation ranged between $120 \pm 4\%$ and $238 \pm 20\%$ (Table 3). Genes showing down-regulation included the following categories: (a) catecholaminergic, (b) chemokine and their receptors, (c) death factors, (d) immediate early genes, (e) Rho-GTPase effector, (f) transporters, and (g) tyrosine kinases. The down-regulated values ranged between $21 \pm 3\%$ and $84 \pm 3\%$. Other gene groups had both up and down-regulated expression values. The details about the genes persisted at both time points are given in Table 4.

3.5. *Gene that was close to 0.05 level significance (but were not included in the list) in the late time point*

Because of to the very close proximity to the statistically significant level of 0.05, brain nitric oxide synthase was analyzed further for their physiological relevance. This gene was up-regulated $136 \pm 3\%$.

3.6. *Principal component analysis of the gene expression*

The results of the PCA analysis are shown in Fig. 7. In this three-dimensional graph we see that controls (C1, C2, C3) for early time point (15 min) were different from the treated animals (T1, T2, and T3). It is interesting to note that controls (C7, C8, C9) of the late time point (3 months) were separating distinctly, not only the treated groups (T7, T8 and T9), but also from both of the treated (T1, T2 and T3) and control groups (C1, C2 and C3) at early time point. There was a clear difference between the early time point gene expression pattern for each animal (representing both control and treated groups) and that of the control and treated animals at the late time point, thus confirming the evolution of toxicity-related gene expression as a function of age and dose.

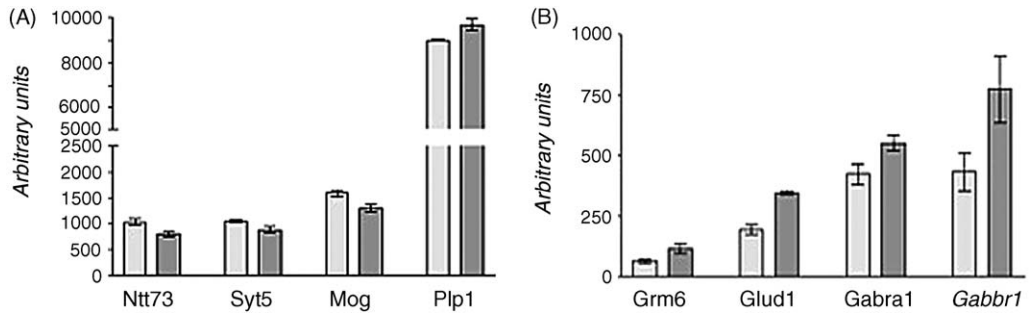

Fig. 4 – Histograms showing the mRNA expression levels at 15 min post-treatment time point for various genes belonging to following categories: (A) myelin proteins and neurotransmitter transporters; (B) glutamergic and GABAergic signaling. Arbitrary units of fluorescent hybridization data obtained from both control (clear) and treated (shaded) sets for each gene are included in this figure. All data in this figure passed the 0.05 level of statistical significance.

Table 2 – Fifteen minutes sarin treated microarray data

Probe ID		Gene symbol	mRNA modulation (percent control)
ATPases and ATP-based transporters			
JO4963	Ecto-ATPase (carcinoembryonic antigen-related cell adhesion molecule 1)	Ceacam1	334 ± 5
Calcium channels and binding proteins			
M92905	Calcium channel alpha-1 subunit	Cacna1d	59 ± 7
D86556	Ca^{2+}/calmodulin-dependent protein kinase I beta	Camk1b	160 ± 9
AF027984	Low voltage-activated, T-type calcium channel, alpha subunit	Cacna1g	117 ± 5
L13406	Calcium/calmodulin-dependent kinase II delta subunit	Camk2d	70 ± 3
Catecholaminergic signaling			
M84009	Dopamine receptor D4 (RATD4)	Drd4	225 ± 3
Chemokines and their receptors			
Y13400	Receptor protein CKR3	Cmkbr3	282 ± 1
U90610	CX-C chemokine receptor	Cxcr4	118 ± 4
rc_AA8006	CX-3C chemokine (small inducible cytokine subfamily D, 1)	CX-3C, Scyd1	194 ± 1
rc_Al01409	Lymphotactin (small inducible cytokine subfamily C, member 1)	Ltn, Scyc1	127 ± 6
Cholinergic signaling			
U42976	Neuronal nicotinic acetylcholine receptor subunit beta4	Chrnb4	150 ± 9
J03025	Muscarinic cholinergic receptor	Chrm2	214 ± 2
Cyclic nucleotide signaling			
M25348	Cyclic nucleotide phosphodiesterase (PDE2)	PDE2	38 ± 1
Cytokines and their receptors			
X60675	Interleukin 10	IL10	156 ± 16
Cytoskeletal and cell adhesion molecules			
M34384	Nestin	Nes	133 ± 5
U67140	PSD-95/SAP90-associated protein 4	Psd95/Sap90	135 ± 5
AB011679	Class I beta tubulin	Tubb1	67 ± 4
D14048	SP120	Hnrpu	57 ± 9
M96853	Postsynaptic density protein (PSD-95), discs-large tumor supressor homolog	Sap90, Dlgh4	140 ± 1
M96375	Non-processed neurexin 1-beta	Nrxn-1b	74 ± 3
S73007	Synuclein SYN1 {alternatively spliced} [rats, mRNA, 695 nt]	Snca	78 ± 6
rc_Al14601	Non-processed neurexin 1-alpha	Nrxn-1a	81 ± 3
Detoxification molecules			
S72505	Glutathione S-transferase Yc1 subunit [rats, fetal liver, mRNA, 1052nt]	Gsta2	71 ± 2
Energy metabolism			
D30666	Brain acyl-CoA synthetase II (fatty acid Coenzyme A ligase, long chain 3)	Facl3, Acs3	82 ± 3
D45862	Obesity (leptin)	Lep, OB	162 ± 3

Table 2 (*Continued*)

Probe ID		Gene symbol	mRNA modulation (percent control)
GABAnergic signaling			
AB016161	Gabab receptor 1d	Gabbr-1	179 ± 2
LO8490	GABA-A receptor alpha-1 subunit	Gabra1	130 ± 5
Glutamergic and aspartate signaling			
D13963	Metabotropic glutamate receptor subtype	Grm6	177 ± 2
rc_Al13742	Glutamate dehydrogenase	Glud1	178 ± 2
G-protein coupled receptor pathway-related molecules			
U30290	Galanin receptor GALR1 mRNA	Galr1	278 ± 5
L27487	Calcitonin receptor-like receptor (CRLR)	Calcrl	86 ± 6
rc_Al13606	Beta-arrestin	Arrb-1	133 ± 6
Growth factors			
J00739	Growth hormone	Gh	156 ± 2
X07285	Basic fibroblast growth factor	Bfgf	161 ± 1
X16703	Insulin-like growth factor II	Igf2	167 ± 2
Immediate early genes			
AF050661U	Activity and neurotransmitter-induced early gene 9 (Ania-9)	Ania-9	225 ± 5
Ion channels			
S64320	Shal1=K+channel polypeptide [rats, hippocampus, mRNA, 3350 nt]	Kcnd	138 ± 7
M26643	Skeletal muscle voltage-sensitive sodium channel alpha subunit	Scn4a	338 ± 3
U93052	Ca^{2+}-activated K^+ channel alpha subunit (large conductance)	Kcnma1	331 ± 4
D13985	Chloride channel, nucleotide sensitive	Clns1a	177 ± 2
U69882	Ca^{2+}-activated K^+-channel rSK2 (SK), small conductance subfamily N, 2	Kcnn2	64 ± 3
Z56277	CLC-5 chloride channel	Clcn5	146 ± 9
U72410	Kir3.1 alternate splice variant deltaB, inwarding rectifying, subfamily J, 3	Kcnj3	199 ± 3
Y14635	Proton-gated channels modulatory subunit (degenerin)	Accn1	129 ± 6
Mitochondria-associated proteins			
S76511	Bax apoptosis inducer [rats, ovary, mRNA partial, 402 nt]	Bax	75 ± 5
AF027954	Bcl-2-related ovarian killer protein (Bok)	Bok	70 ± 7
Mitogen activated protein cascade molecules			
rc_Al17883	MAP kinase kinase	Map2k	132 ± 6
Myelin proteins			
M99485	Myelin oligodendrocyte glycoprotein (MOG)	Mog	82 ± 3
rc_Al07277	Lipophilin	Plp1	108 ± 2
Neurotransmission and neurotransmitter transporters			
S56141	Sodium-dependent neurotransmitter transporter {clone vta 1732}	Ntt73	77 ± 3
U26402	Synaptotagmin 5	Syt5	84 ± 3
Neuropeptides and their receptors			
E05551	Receptor of vasoactive intestinal polypeptide (VIP)	Vipr	219 ± 2
U09631	VIP2 casoactive intestinal polypeptide receptor	Vipr2	96 ± 8
S39779	Preproendothelin-3 [rats, mRNA, 734 nt]	Edn3	236 ± 8
S49491	Proenkephalin [rats, heart, 1250 nt]	Penk-rs	63 ± 2
AF041244	Hypocretin (orexin) receptor-1	Hcrtr1	139 ± 4
Nitric oxide signaling			
AF006619	Dahl/Rapp S (salt-sensitive) nitric oxide synthase (Nos-2)	Nos-2a	167 ± 1
Purinergic signalling molecules			
M64299	A1 adenosine receptor	Adora1	201 ± 1
X80477	P2X purinergic receptor, ligand-gated ion channel, 1	P2rx1	193 ± 2
AF020756	P2X2–3 receptor, ligand-gated ion channel, 2	P2rx2	151 ± 1
Serotonergic signaling			
S62043	Serotonin receptor, histamine H2R homolog [rats, striatum, mRNA, 1929 nt]	Htr6	47 ± 8
X63995	Serotonin neurotransmitter transporter	Slc6a4	141 ± 9
TNF beta family molecules			
L00981	Lymphotoxin (TNF-beta)	Lta, Tnfb	195 ± 5
Transcription factors			
L13206	HNF-3/fork-head homolog 6 (HFH-6)	Foxd4	170 ± 7

Table 2 (*Continued*)

Probe ID		Gene symbol	mRNA modulation (percent control)
Tyrosine phosporylation molecules			
D12524	C-kit receptor tyrosine kinase	Kit	23 ± 2
U21954	Tyrosine kinase receptor Ehk-3, full length	Epha7	238 ± 3

Table 3 – Three months sarin treated microarray data

Probe ID		Gene symbol	mRNA modulation (percent control)
Calcium channels and binding proteins			
J02942	Calcium/calmodulin-dependent kinase type II-alpha subunit	CamkIIa	21 ± 3
U49126	Neuroendocrine calcium channel alpha 1 subunit, variant CaCh3	CaCh3	220 ± 0
M89924	L-type voltage-dependent calcium channel (VDCC), alpha 1 subunit	Cacna1c	149 ± 6
AA957510	Alternative brain Ca^{2+} transport ATPase 2	Atp2a3	79 ± 5
Catecholaminergic signalling			
M93257	Cathecol-O-methyltransferase	Comt	39 ± 1
Chemokines and their receptors			
AF0058	Chemokine CX-3C	Scyd1, CX-3C	56 ± 1
Cyclic nucleotide signaling			
M25348	Cyclic nucleotidephosphodiesterase (PDE2)	PDE2	120 ± 4
U12623	Cyclic nucleotide gated cation channel	Cgn2	238 ± 2
Cytokines and their receptors			
M26745cds	Interleukin 6 (IL6)	IL6	168 ± 1
L36460	Interleukin-9 (IL-9) fragment	IL9	223 ± 0
Cytoskeletal and cell adhesion molecules			
U30938	Microtubule-associated protein (MAP2)	Map2	140 ± 1
M96375	Non-processed neurexin 1-beta	Nrxn-1b	73 ± 4
Al171319	SW1/SNF related matrix associated actin dependent regulator of chromatin	SW1/SNF	171 ± 2
Death factors			
AF053362	Death effector domainn-containing protein DEFT	Dedd, deft	48 ± 9
GABAnergic signaling			
X51991	GABA A receptor alpha-3 subunit	Gabra3	166 ± 2
AB016161	Gabab receptor 1d	Gabbr-1d	65 ± 6
X15468	GABA(A) receptor beta3 subunit	Gabrb3	67 ± 6
G-protein coupled receptor molecules and regulators			
rc_Al013765	beta-arrestin	Arrb-1	128 ± 6
Glutamergic and aspartate signaling			
X17184	Glutamate receptor, AMPA subtype, GluR1	Gria1	236 ± 1
Growth factors and inhibitors			
X59290	eek (eph and elk-related kinase)	eek	180 ± 2
Z11558	Glia maturation factor beta (GMF-beta)	Gmfb	164 ± 1
AA924772	growth inhibitory factor - metallothionein homolog	Gif-Mt	144 ± 1
Immediate-early genes			
X17163	C-jun oncogene for transcription factor AP-1	Jun	33 ± 8
X06769	C-fos	Fos	34 ± 1
AF050661	Activity and neurotransmitter-induced early gene 9 (Ania-9)	Ania-9	42 ± 1
AF030087	Activity and neurotransmitter-induced early gene 2 (Ania-2)	Ania-2	66 ± 8
Ion channels			
U53211	Neuronal degenerin channel MDEG	Accn1	130 ± 3
AF000368	Voltage-gated sodium channel	Scn9a	47 ± 6
Metabolism			
rc_Al227665	Phosphatidylserine decarboxylase	PISD	154 ± 6
Neuropeptides and their receptors			
J05189	Neuromedin K receptor	Tacr3, Nmkr	70 ± 5
X01032	Cholecystokinin C precursor	Cck	126 ± 5

Table 3 (*Continued*)

Probe ID		Gene symbol	mRNA modulation (percent control)
Proteases			
D14478	Pre-mature calpain	Capn8	230 ± 5
Rho-GTPase effector			
AF021935	Mytonic dystrophy kinase-related Cdc42-binding kinase	PK428	60 ± 2
Synaptic vesicle proteins			
AJ006855	Synaptojanin 1	Synj1	84 ± 3
rc_AA799879	Synaptogyrin 1	Syngr1	131 ± 5
Transporters			
M58040	Transferrin receptor	Tfrc	74 ± 5
D13962	Neuron glucose transporter	Slc2a3, Glut3	78 ± 4
Tyrosine kinases			
rc_Al237836	XLA alpha	Btk	82 ± 4

3.7. *Tree view and clustering analysis*

The graphic representation of the data for both early and late time points is given in the Fig. 8. Most of the down- and up-regulated genes clustered at top and lower portion of the tree view, respectively. The remarkable homogeneity of the coloring pattern validates the reproducibility of the replicate data from both the control and treated groups.

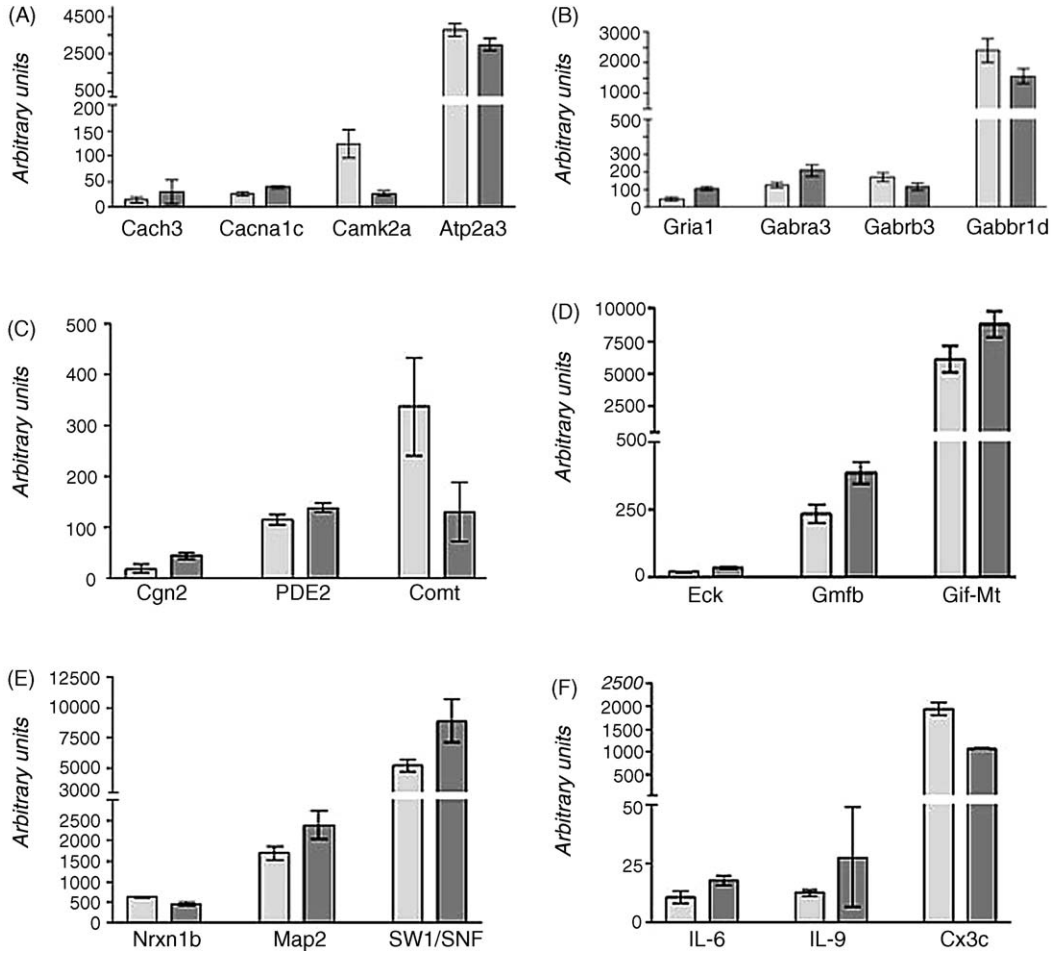

Fig. 5 – Histograms showing the mRNA expression levels at 3 months time point for various genes belonging to following categories: (A) calcium channel and binding proteins; (B) GABAergic and glutamergic signaling; (C) cyclic nucleotide and catecholaminergic signaling; (D) growth factors and inhibitors; (E) cytoskeletal and cell adhesion molecule; (F) cytokines and cytokine receptors. Arbitrary units of fluorescent hybridization data obtained from both control (clear) and treated (shaded) sets for each gene are included in this figure. All data in this figure passed the 0.05 level of statistical significance.

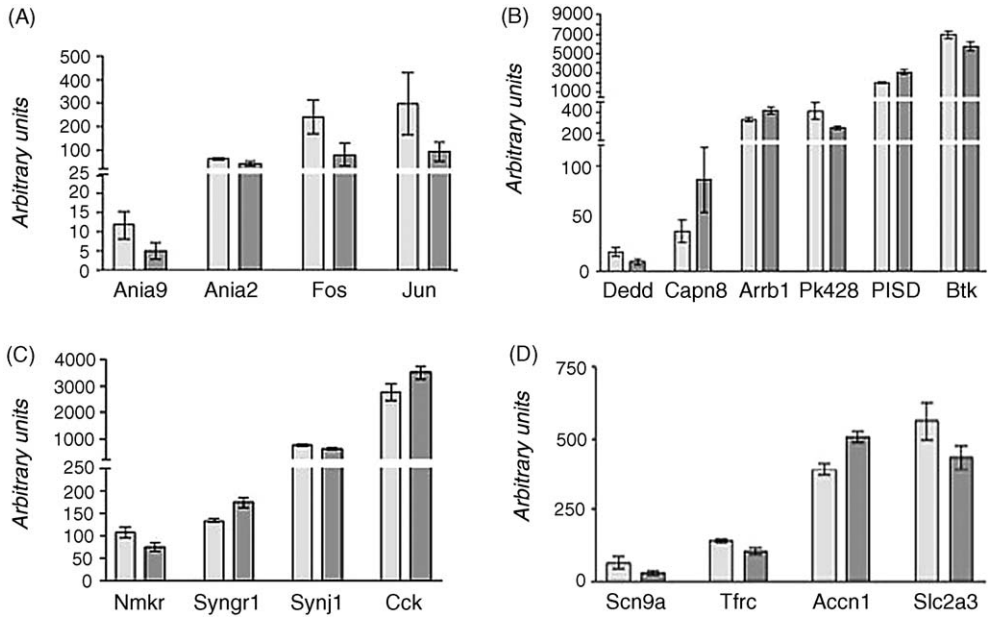

Fig. 6 – Histograms showing the mRNA expression levels at 3 months time point for various genes belonging to following categories: (A) immediate early genes; (B) miscellaneous group, containing genes belonging to death factors (Dedd), proteases (Capn8), G-protein coupled receptor molecules and regulators, (Arrb-1), Rho-GTPse effector (PK428), phosphatidylserine decarboxylase (PISD), and tyrosine kinase (Btk); (C) neuropeptide signaling and synaptic transmission; (D) ion channels. Arbitrary units of fluorescent hybridization data obtained from both control (clear) and treated (shaded) sets for each gene are included in this figure. All data in this figure passed the 0.05 level of statistical significance.

3.8. *Gene expression validation*

In this semi-quantitative approach, the expression data obtained for each of the following genes were normalized to values obtained for the 18S RNA data. The gel picture consisting of representative PCR bands of the RT-PCR experiments from control and treated groups is given in Fig. 9. Details of the validation data as compared with array data are provided in Table 5. The validation data showed the same trend observed in the array analysis. Increased levels of the transcripts in the validation for some genes can be attributed to increased sensitivity of the PCR approach.

3.9. *CamkIIa expression in different regions of the brain at 24 h*

CamkIIa was selected to study the expression pattern in different regions such as the cortex, brainstem, midbrain and cerebellum, to validate our approach that total brain gene expression studies could still identify key genes, in spite of differential alteration in specific regions of the brain. The cortex and midbrain showed down-regulated expression of CamkIIa (35 ± 3% and 62 ± 6%, respectively in Fig. 10A and B), while the brainstem and cerebellum showed up-regulation of the CamkIIa transcript levels (140 ± 5% and 182 ± 2%,

Table 4 – Persistence of altered expression of specific genes at early (15 min) and late (3 months) time points

Name of the Gene	Early time point (%)	Late time point (%)
Ania-9	225 ± 5	42 ± 1
Arrb-1	133 ± 6	128 ± 6
CX-3C	194 ± 1	56 ± 1
Gabab-1d	179 ± 2	65 ± 6
Nos-2a	167 ± 1	136 ± 3
Nrxn-1b	74 ± 3	73 ± 3
PDE2	38 ± 1	120 ± 1

Table 5 – Expression validation data (relative RT-PCR) as compared with array data

Gene	Array data		Relative RT-PCR	
	Early	Late	Early	Late
Ania-9	225 ± 5%	42 ± 1%	261 ± 5%	43 ± 3%
Arrb-1	133 ± 6%	128 ± 6%	152 ± 2%	129 ± 3%
CamkIIa	CL[a]	21 ± 3%	CL[a]	25 ± 2%
Camk2d	70 ± 3%	CL[a]	66 ± 2%	CL[a]
Chrm2	214 ± 2%	CL[a]	224 ± 3%	CL[a]
Chrnb4	150 ± 9%	CL[a]	164 ± 3%	117 ± 3%
CX-3C	194 ± 1%	56 ± 1%	219 ± 1%	52 ± 3%
Gabbr-1	179 ± 1%	65 ± 6%	199 ± 6%	71 ± 3%
IL-10	156 ± 1%	CL[a]	161 ± 3%	CL[a]
Map2	CL[a]	140 ± 1%	CL[a]	141 ± 2%
Nes	133 ± 5%	CL[a]	148 ± 4%	CL[a]
Nos-2	167 ± 1%	136 ± 3%	182 ± 2%	145 ± 2%
Nrxn-1b	74 ± 3%	73 ± 4%	52 ± 4%	49 ± 2%
PDE2	38 ± 1%	120 ± 4%	49 ± 3%	125 ± 4%
Synj1	CL[a]	84 ± 3%	CL[a]	77 ± 6%
Beta-actin	CL[a]	CL[a]	CL[a]	CL[a]
18S RNA	CL[a]	CL[a]	CL[a]	CL[a]

[a] CL: control levels.

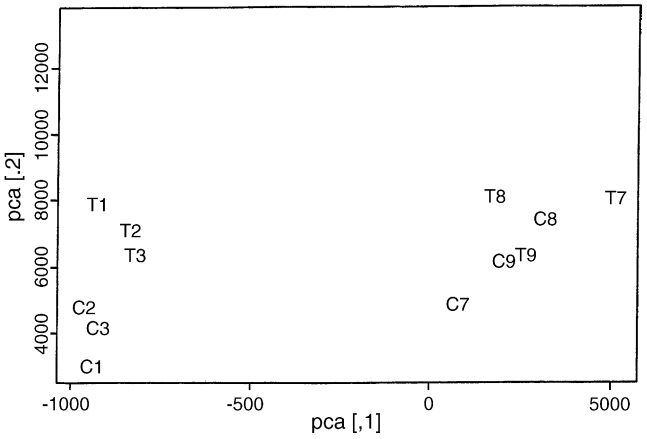

Fig. 7 – Principle component analysis (PCA) of gene expression was prepared in a three dimensional platform and presented here as a graph providing a global view on the differences and similarities among groups and individual animals. C1, C2, and C3 as well as T1, T2, and T3 represent the total gene expression profile (sum of all gene expressions, where gene expression for every gene is estimated with an assigned weight) for control and treated group animals, respectively at 15 min time point. Similarly, global gene expression profile for controls (C7, C8, C9) and treatment groups (T7, T8, 79) of three months time point were measured and compared with 15 min time point. It is interesting to note that controls (C7, C8, C9) of the late time point (3 months) were separating distinctly, not only from its treated groups (T7, T8 and T9), but also from both the treated (T1, T2 and T3) and control groups (C1, C2 and C3) of early time point. Both time points represent different doses also (15 min being 0.5 × LD_{50}, while 3 months time point represent 1 × LD_{50} dose of sarin).

respectively in Fig. 10C and D). It can be understood that since both cortex and midbrain together constitutes a larger part of the total brain as compared to the combined area of brainstem and cerebellum, the overall pattern of the total brain RT-PCR validation experiment resembles that of the cortex and midbrain (21 ± 3% at 3 months from this study; 56 ± 1% at 2 h from a related study [36]).

4. Discussion

Organophosphates such as sarin elicit their acute toxic effects by irreversible inhibition of acetylcholinesterase and excessive stimulation of postsynaptic cholinergic receptors. This is followed by the activation of glutamate receptors leading to the release of the excitatory L-glutamate amino acid neurotransmitter (De Groot, 104). This in turn activates *N*-methyl-D-aspartate (NMDA) subtype of glutamate receptor and the opening of NMDA Calcium channels, resulting in massive Ca^{2+} influx of post synaptic cell causing neuronal degeneration [39,40]. Organophosphate-induced cholinergic effects are usually manifested immediately following high level exposure [3,41]. There are numerous studies in both

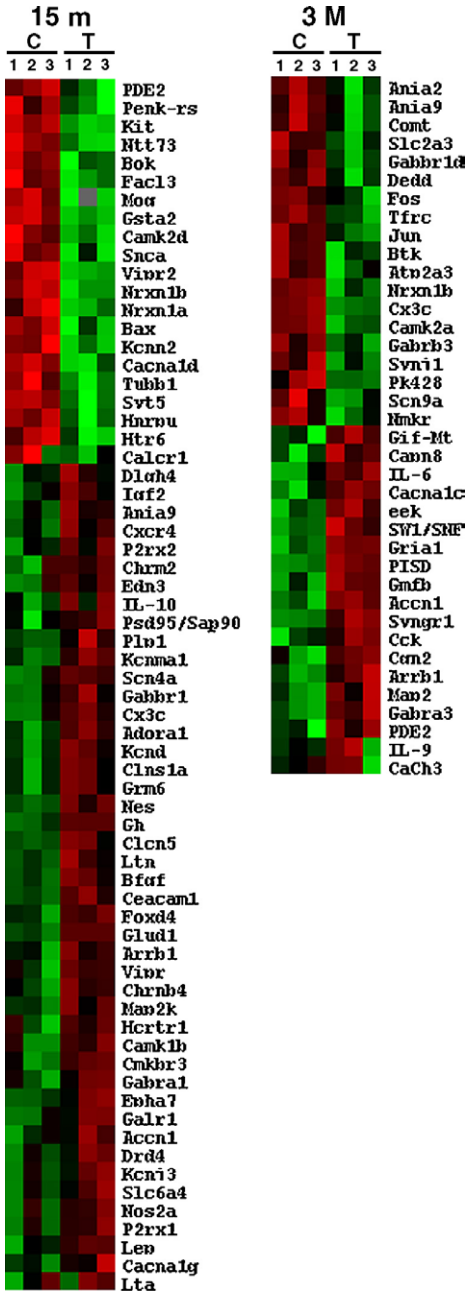

Fig. 8 – Tree view analysis of gene expression from both time points is presented here. The analysis was done using publicly available software and analysis was done for each time point separately and clustered according to gene expression and not per experiment. Both figures show that most of the down-regulated genes (green color in the treated and red color in the control) were clustering on top of the tree view, while the up-regulated genes (red color in the treated and green color in the control) cluster at the lower portion of the tree view. The remarkable homogeneity of the coloring pattern validates the reproducibility of the replicate data from both control and treated groups.

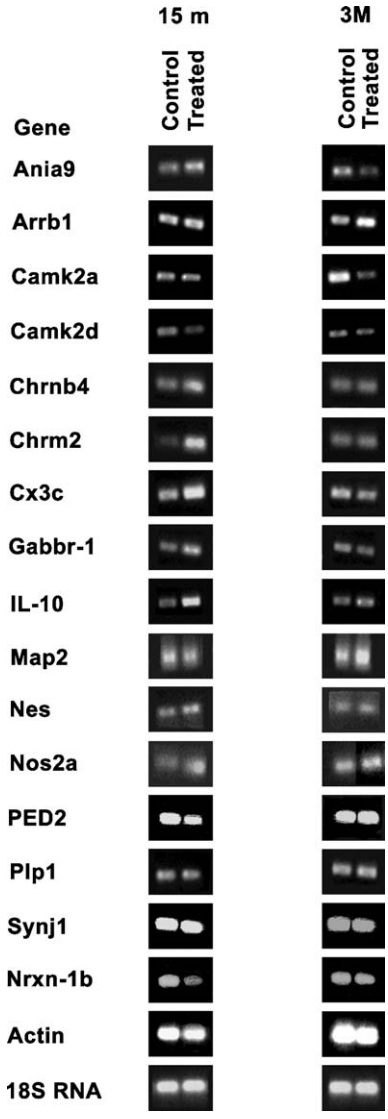

Fig. 9 – Gel pictures of representative RT-PCR products of validated genes from control and treated groups (selected from three animals in each group) of early (15 m: fifteen minutes) and late (3 M: three months) time points are shown here. An agarose gel (2%) was prepared 1 × TAE buffer and PCR products were run in the same buffer for 2 h at 70 V.

humans and animals showing that survivors of high-level organophosphate exposure can experience subtle but significant long-term neurological and neurophysiological outcomes that are detectable months or even years following the acute exposure, that has been characterized as organophosphorus ester-induced chronic neurotoxicity (OPICN) [42]. Although the mechanisms of the chronic neurotoxicity is yet to be defined, available data suggest that it involves apoptotic neuronal cell death, similar to that proposed following cell exposure to micromolar concentrations of L-glutamate [43]. Also, increased AChE expression following sarin exposure [20] might induce apoptotic cell death similar to that proposed for Alzheimer Disease [44]. This suggestion is in agreement with the finding that AChE was toxic to neuronal (Neuro 2a) and glial-like (B12) cells [45].

High throughput studies of gene expression may result in the identification of genes that are differentially regulated in toxicant-induced disease/syndrome state. This may be useful for two main reasons: (1) these genes may form the basis for a diagnostic test. For example, if some differentially regulated genes are expressed in peripheral tissues such as blood, then a test for a brain dysfunction due to toxicant exposure may be developed. This may be useful for early pharmacological intervention: (2) abnormally regulated genes in the treated samples may be dynamically altered in response to the disruption of a particular biochemical pathway in affected cells and may represent secondary changes in the disease state that reflect the essential pathway whose function has been compromised in the disease state. Such genes identified as abnormally regulated using microarray technology may suggest potential therapeutic targets. Judging from the variety of gene expression changes, we have found that were hitherto unknown, the current study attempts to highlight the above-mentioned objectives.

This report is the first of its kind to provide molecular evidence for the sequence of events that occurs either concurrently or in quick succession in sarin-induced neurotoxicity in the rat CNS. This report also confirms for the first time that many signaling pathways were altered within the first 15 min after acute sarin exposure and thus many genes behave as immediate early response genes to the toxic stimuli.

Contrary to the conventional belief, sarin treatment altered several major pathways in the CNS such as cyclic nucleotide signaling, catecholaminergic signaling, GABAergic signaling, glutamate and aspartate signaling, nitric oxide signaling, purinergic; serotogenic, as well as cholinergic signaling, all at a sub-lethal dose ($0.5 \times LD_{50}$) and immediately (within the first 15 min). Other signal transduction pathways such as calcium channels and binding proteins, ligand-gated ion channels, neurotransmission and neurotransmitter transporters, neuropeptides, TNF pathways, chemokines (such as CX-C members), and cytokines (such as IL 10) were also altered within 15 min (Table 2).

4.1. *Sarin-induced alterations in gene expression related to electrophysiological activities of the CNS*

Abnormal electrophysiological recordings in rhesus monkeys [46] and neuropathy in rats [16,17] following a single large dose or repeated sub-clinical doses of organophosphates have been reported. High concentrations of organophosphates have been reported to affect excitable membranes directly, by blocking peripheral nerve conduction [47]. High-level induction of a very large group of ion channel-related genes, i.e., sodium, potassium, chloride and proton-gated (Table 2) indicates severely altered electrophysiology at the15 min time point. On the other hand, only two genes (Accn1 and Scn9a) showed persisting alterations at 3 months, supporting the notion that sarin-induced electrophysiological changes initiated early were minimized, but not completely normalized. Brain neuronal degeneration and other problems related to memory and other defects, characteristic of OPICN, reported by the Gulf

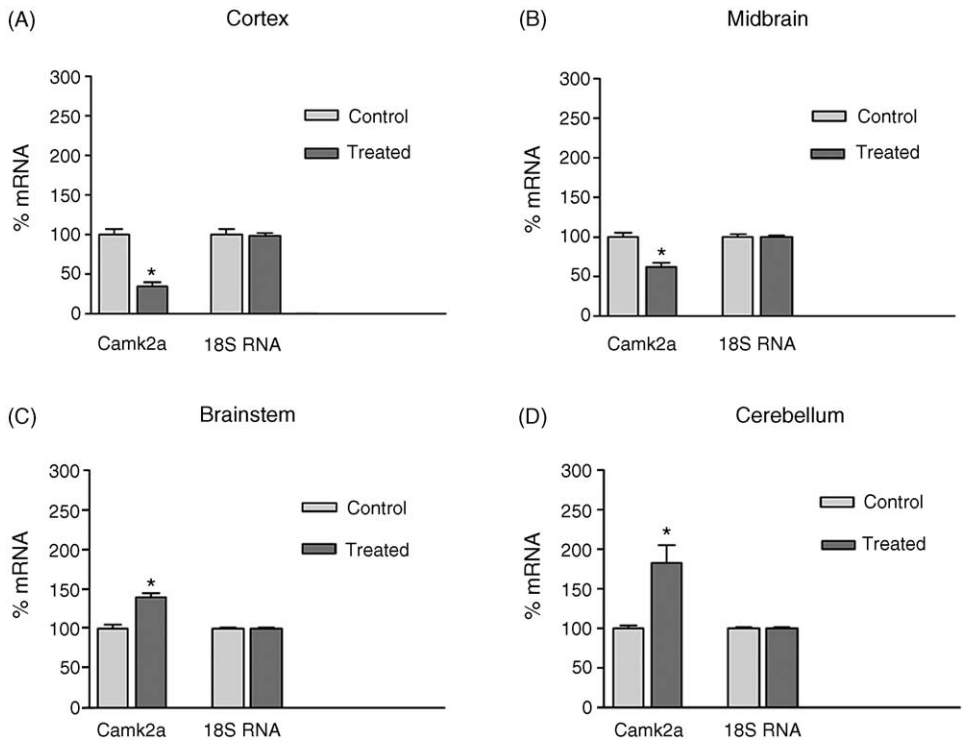

Fig. 10 – This figure shows the data on the level of CamkIIa mRNA expression from different regions of the brain such as cortex, midbrain, brainstem, and cerebellum in sarin-treated (0.05 × LD_{50}) animals. Total RNA was extracted from different regions of the brain from control and treatment groups (each three animals) were subjected to cDNA synthesis using olgo-dt primers and PCR reaction with CamkIIa-specific primer sets. 18S RNA was used as a control for normalizing the data. The data shown here in the histograms represent percentage values where the control values constituted 100%. Statistical analysis was done using student's *t*-test. Both cortex and midbrain showed down-regulation of the CamkIIa levels, while cerebellum and brainstem showed induction of the transcript levels for CamkIIa. Overall trend of gene expression from these distinct regions of brain resembled the pattern observed for total brain array data at 3 months.

War veterans and the victims of the sarin terrorists' attack in Japan could account for such persistence of electrophysiological anomalies. Finding the highest expression of Ecto-ATPase at 15 min and the persistence of altered levels of several other ATPases and ATP-based transporters at the 2 h time point [36] as well as at 3 months (Table 3) support the idea that early perturbations in CNS electrophysiology persist for a long time after the initial acute sarin-exposure event.

4.2. *Sarin-induced alterations in growth factor-related genes*

Rat growth hormone, basic fibroblast growth factor, and insulin-like growth factor-II were found to be induced at 15 min, while growth factors related to glial function (Gmfb), eek (eph and elk-related kinase) and growth inhibitory factor-metallothionein homolog (Gif-Mt) were induced at 3 months. Alterations induced by DFP (a structural analogue of sarin), of NGF (neural growth factor) in the SK-5-SY cell line, indicate a role for NGF-mediated pathways by organophosphates [48]. There are no reports on the direct roles of other growth factors implicated in sarin-induced neurotoxicity. DFP; however, has been shown to reduce serum prolactin, thyropton, luteinizing hormone, and growth hormone, and increase adenocorticotropin and corticosterone in rats, indicating a multiplicity of effects on anterior pituitary function by organophosphates [49].

The role of FGF in early rodent CNS development and in adulthood [50–53] is well- known. It is also interesting to note that those cells stimulated by bFGF, also showed robust expression of nestin which plays role in the neuronal and glial differentiation of bipotential cells [53]. Induction of both nestin and bFGF in sarin-treated CNS at 15 min, indicates a protective mechanism either by inducing the proliferation or increasing the differentiation of bipotential cells into neurons or glia, as and when required at distinct regions of the damaged CNS.

4.3. *Sarin-induced oxidative stress, lipid peroxidation and cell death/neuroprotection-related gene expression*

Many pesticides including organophosphates and other environmental chemicals including warfare agents (like sarin) have been implicated in oxidative stress-mediated free radical generation and alterations in the anti-oxidative scavenging system [54]. We have seen an induction of Nos-2 mRNA expression at the early time point, which is consistent with our previous finding of the production of nitrotyrosine in rats exposed to sarin [55]. Gupta et al. have found an

inverse relationship between the NO increase and a decrease in high-energy phosphates in DFP-treated rat CNS and they have attributed that to NO-induced impaired mitochondrial respiration leading to depletion of energy metabolites [56]. Alteration in the levels of brain Acyl-CoA synthetase and Leptin accompanied by a decrease in the mRNA levels of key mitochondria associated proteins such as Bax (apoptosis inducer) and BOK (BCL-2 related ovarian killer protein) strongly supports such an idea. Moreover, apoptosis-related genes such as Bcl-X beta and BOD-M were also found to be altered at 2 h [36]. These chemicals may alter cytochrome P-450 (as in this study), and in their metabolic process, oxidants are generated that are capable of oxidizing a wide range of endogenous chemicals and xenobiotics [57]. Persistent alteration in the cell death-related molecule DEFT at 3-month adds strength to the notion that oxidative stress-related changes can cause long term complications in cell physiology and pathology. ROS have been shown to increase production of cytokines such as TNF-α [58], chemokines such as IL-8, and adhesion molecules (ICAM)-1 [59]. Our data indicate a very strong induction of TNF-beta (Ltn) at 15 min, while CX-3C was down-regulated at 15 min and also at 3 months. Many cell adhesion and cytoskeleton-related molecules showed alteration at 15 min of which some were related to BBB function (neurexin 1-beta; neurexin 1-alpha, PSD-95/SAP90-associated protein 4), while others are well characterized cytoskeleton genes (Nestin, beta tubulin). Persistence of Neurexin 1-beta at 3 months might indicate a continued a dysfunctional BBB and continuing perturbed oxidative stress-related phenomena.

Lipid peroxidation due to sarin treatment is indicated by the alteration in the lipophilin gene expression, while the involvement of iron free radicals in the long term damage is indicated by the persistent alteration noted for 'transferrin' receptor and the consequent defects in the neuronal glucose transport by the altered 'Neuron glucose transporter' at the 3 months time point. Lipid peroxidation has been shown to be present in the CNS of rats treated with sarin [60]. Thus, our results confirm sarin-initiated lipid peroxidation as an important by-product of oxidative stress.

Reduction in glutathione levels, as indicated by the down-regulated mRNA expression profile of this molecule, may potentiate damage to both dopamine and GABA populations, as indicated by the alteration in the mRNA expression of key molecules belonging to these populations (Dopamine receptor type 4 and GABA receptor, respectively). The glutathione system, which is responsible for removing H_2O_2 and maintaining protein thiols in their appropriate redox state in the cytosol and in mitochondria, is an important protective mechanism for minimizing oxidative damage. The cause-effect relationship among energy impairment, glutathione reduction and the loss of dopamine/GABA neurons in the CNS of sarin-treated animals as well as the potential role of NMDA receptor (as indicated by its altered levels) are not yet fully understood. Numerous studies on toxicant-induced changes [61] as well as in several neurological diseases (such as Parkinson's disease [62]); however, indicate an important causative role in the long-term pathological consequences of acute early exposure.

4.4. *Blood brain barrier (BBB) damage and alterations in gene expression*

The BBB maintains the homeostasis of the CNS environment to ensure proper function [63]. Disturbed BBB-related function was indicated by altered levels of MOG, PSD-95, and neurexin. In a recent study from our laboratory, we have shown that large toxic doses of sarin caused breakdown of the BBB [17] and that BBB disruption played an important role in the sarin-induced cell death in the motor cortex, hippocampus and cerebellum. Sarin-induced death of the motor cortex could lead to motor and sensory abnormalities, ataxia, weakness and loss of strength. Furthermore, hippocampus degeneration leads to learning and memory deficits. Lesions in the cerebellum could result in coordination abnormalities.

Within 15 min of exposure, kinase cascades such as CamkII and MAP kinase kinase were altered in cell types that compromise the BBB, within 15 min, which probably received transducing signals due to changes seen in several sources such as growth hormones, and other growth factors such as IGF 2 and bFGF as identified in this study. The next logical step in this kinase cascade could be tyrosine phosphorylation, which might increase tight junction permeability [64]. In the present study, we noted that tyrosine kinase receptor EHK-3 was up-regulated, supporting such hypothesis. That such phosphorylation might be actively involved in regulating BBB transport processes is evident from our observation that transporters such as sodium-dependent neurotransmitter transporters and ATP-based transporters were also shown to be altered. The change in the BBB could also be indicated by the over-expression of preproendothelin (EDN 3). A primary mediator of injury-induced BBB disruption is nitric oxide (NO). Induction of nitric oxide synthase along with the changes in EDN 3 expression indicates such a scenario. Agents that regulate vasoactive processes, such as vasoactive intestinal receptor-1 (Vipr 1) and 2 (Vipr 2) might be involved in the biochemical opening of the BBB, as shown earlier for other vasoactive genes such as braykinin and angiostensin [65].

Changes noted in the NMDA receptor function-related genes in the current study also are interesting. For example, the expression levels of postsynaptic density 95 (PSD-95) as well as PSD-95/SAP-90-associated protein, were up-regulated at the early time point, along with NMDA and Nos-2a synthase levels. PSD-95 participates in the anchoring of the NMDA receptor and interacts with neuronal NO synthase at the postsynaptic membrane and thereby plays a fundamental role in synaptic transmission and memory formation [66]. Altered levels might explain an early abnormal event that might have initiated complex processes leading to the memory loss observed in sarin exposed rats [67]) and in Gulf War veterans at a later time point. This also confirms the recent observation by Kim et al. [68] about the role of NOS/NMDA-mediated apoptosis in the DFP-treated rat CNS. As mentioned earlier, persistence of altered expression of BBB-related molecules such as Neurexin-1 beta thus adds strength to our hypothesis that early lesions lead to permanent damage at a later time point.

4.5. *The cholinergic system and sarin-induced gene expression*

Numerous studies from our group and others have shown that excessive accumulation of acetylcholine leads to activation of ligand-gated ion channels, and of nicotinic acetylcholine receptors (nAChR) and muscarinic acetylcholine receptors (mAChE), which activate diverse kinds of cellular response by distinct signaling mechanisms [69]. Immediate over-expression of the M2 receptor gene confirms our earlier biochemical data, showing consistent alterations in receptor density at 1, 3, 6, 15, and 20 h post-treatment [60]. Nicotinic acetylcholine receptors are essential for neuromuscular signaling and are also expressed in non-neuronal tissues, where their function is less clear. Nicotinic acetylcholine receptors in neurons alter apoptotic signaling, protecting against cell death in some settings, and this action may in some cases be directed through alternative signaling pathways, including synapse formation. The induced levels of nicotinic acetylcholine receptor probably indicate that it plays a role in all of the above-mentioned capacities. Our expression data, indicating more pronounced over-expression m2-mAChR and nAChR clearly correlates with our earlier findings on increased nAChR and m2-mAChR ligand binding densities [70] in sarin-induced neurotoxicity. Recently, it has been reported that activation of α7 nAChR by a peptide derived from AChE, resulted in the activation of NMDA receptors, calcium release, mitochondrial dysfunction, and production of free radicals, leading to apoptotic cell death [71].

4.6. *G-protein receptors and arrestin-mediated pathways in sarin-induced changes*

Over expression of either β-arrestin 1 or β-arrestin 2 has been demonstrated to augment the desensitization and internalization of several GPCRs [72,73]. Continued over expression of arrestin at 3 months, along with continued over-expression of several GPCRs belonging to several classes (CamkI and II, M2-AChR, GALR1, CRLR) either at 15 min or 3 months, besides several of the cytoskeletal molecules (nestin, map2, etc., from this study), strongly suggest that sarin-induced hyper-phosphorylation persists until a later time point, thus causing defects in the tissue repair process. These 'turn-off' mechanisms are very important in physiological situations, such as at a synapse where a relatively large concentration of released neurotransmitter can cause a rapid activation of events that control neuronal excitability in the postsynaptic neuron. By ensuring that the activated receptors also rapidly inactivate, the neuron is able to respond to the next wave of released neurotransmitter. For example, in the chronic stage of Chagas disease, (associated with severe cardiomyopathy), circulating antibodies that have agonist-like activity at M2 mAChRs, are postulated to cause a chronic desensitization of the mAChRs and contribute to the functional blockade of these receptors [74]. Such a scenario can be expected for several of the key molecules altered in sarin-induced pathology. Moreover, the M2 receptor has been shown to be interacting with β-arrestin by an agonist-dependent phosphorylation mechanism [75]. Our data confirm the fact that sarin-like compounds increase tyrosine phosphorylation of several proteins in the cytosol fraction of the brain, leading to the activation of c-Jun N-terminal kinase (JNK) and a slight activation of MAPK (mitogen activated protein kinase) in the cytosol [76], as indicated by the altered expression of MAP kinase we saw at15 min.

4.7. *Immediate early genes (IEGs) and sarin-induced neurotoxicity*

Although we have not seen the induction of well known IEGs such as c-fos and c-jun in this study, our previous study with DFP (a structural analogue)showed an induction of both genes within 15–30 min [77,78]. Other genes such as Ania-9 and Scya 2 [36], however, showed immediate induction. The most interesting aspect of this expression profile is that all of these genes showed down-regulation at 3 months (c-fos; c-jun; Ania-9; Ania-2;). It is well known that ITFs (immediately induced transcription factors) and IEGs are among the most rapidly degraded of all proteins suggesting breakdown by the calpain and ubiquitin systems operating through lysosomes and proteosomes [79]. Thus, down-regulation of c-Jun and other IEGs can be caused by (1) successful regeneration or, if this cannot be achieved, (2) a resting atrophic state, or (3) cell death.

4.8. *Calcium and calcium-related gene expression in the sarin-treated CNS*

Calcium, which can induce ITFs, has a function in both neuronal survival and PCD (programmed cell death). Altered levels of calcium and calcium channel-related genes such as Cacna1, Cacna1g, CamkI, and CamkII and the persistence of the alteration of CamkII at 3 months (along with other calcium transporter molecules at 3 months) indicate that calcium induced changes persist for a long time, thus probably playing an important role in sarin-induced pathology. The present results showing differential alterations of CamkII in different brain regions are significant, in the light of its involvement in the mechanism of organophosphorus ester-induced delayed neurotoxicity (OPIDN) [80]. Previous studies from our laboratory have demonstrated increased protein and mRNA expression of CamkII in the regions of the nervous system that exhibit neuronal degeneration, such as the spinal cord, brainstem and the cerebellumin in animals that developed OPIDN [35]. The findings that CamkII was up-regulated in the brainstem and cerebellum and down-regulated in the cortex and midbrain are consistent with the sensitivity and the insensitivity of these regions to OPIDN, respectively [80]. It has been suggested that CamkII, which is integrally involved with glutamate receptors in the processes of learning and memory, is activated by Ca^{2+} influx through NMDA receptors resulting in mitochondrial dysfunction and free radical formation, followed by caspase activation and apoptotic cell death of sensitive regions of the nervous system [71]

4.9. *Inflammation and sarin treatment*

Chemokines are a family of small, secreted proteins with diverse immune and neural functions [81]. Some of them

migrate to the site of injury and CX-3C is one such molecule that showed elevated levels at 15 min and persistent induction levels at 3 months, thus confirming that injury-related gene expression changes were continued for longer than the expected time. Acute stress and other toxicant-altered pro-inflammatory cytokines and chemokine and chemokine receptor messages (IL-10, IL-6, Ltn, Lta, Cxcr4 as noted in this study) have been shown to be altered in various tissues [82]. These molecules are involved in neuroprotection, neurodegeneration and neuronal migration, and hence one can speculate that they may a role in either one or more capacities in sarin-induced neurotoxicity [83]. β-Arrestin, which has been found to be over-expressed both at 15 min and 3 months, also mediates the internalization of CXCR family members [84]. Thus, the pathways initiated at early time points persist to later periods, playing an important role in the pathophysiological and adaptive changes. Rho-GTPase proteins are involved in the induction of integrin-mediated events in surface adhesion and proliferation, thereby contributing to synapse formation and neuronal plasticity [85]. The altered expression of Rho-GTPase effector (PK428) at 3 months, indicating enduring changes in neuronal plasticity.

4.10. *Age and sarin-induced gene expression*

The study of genetic variants in a wide variety of organisms has provided evidence for a major role for oxidative damage as an underlying mechanism of aging [86]. The macromolecular targets of oxidative damage include the following: (a) structural and regulatory genes modulating the genesis of free radicals; (b) structural and regulatory genes for scavenger enzymes; (c) genes regulating the flux of non-enzymatic free radical scavengers; (d) genes regulating target copy number; (e) genes specifying target structure; (f) structural and regulatory genes for repair of target macromolecules; and (g) genes specifying the orderly replacement of effector cells [86]. By looking at the profile one can identify at least one molecule belonging to these different categories involved in the aging process. Hence, sarin-induced oxidative damage may hasten the process of aging, leading to persistence of molecular lesions. The macromolecular targets of oxidative damage include lipids, proteins, and DNA, both mitochondrial and nuclear [87] as discussed earlier.

4.11. *Expression as an indicator of toxicity*

In principle, genes that are directly regulated by sarin should respond more readily than genes that respond due to secondary changes. We also hypothesized that those genes, showing the highest level of up-regulation or down-regulation should also be the key ones that are directly altered by sarin's action. The highest levels of up-regulation were seen for many of the ion-channel related genes, confirming that electrophysiology-related phenomena play a major role in the long-term damage. Of the two cholinergic systems-related molecules, m2-mAChR showed much more pronounced over expression than n-AChR, indicating a more important role for those pathways involved in it. Severe levels of down-regulation of apoptosis-related genes (such as BAX, and BCL-2 as well as PDE2) indicate that these molecules are involved in processes such as cell death and cyclic-nucleotide related metabolism that are directly affected by sarin treatment. On the contrary, the expression profiles from cytoskeletal molecule indicate a mixture of direct and indirect actions by sarin.

4.12. *Persistence of altered expression profiles*

Long-term changes in certain molecules indicate that these molecules play important roles in preserving, amplifying and transmitting the altered expression until a later time point which could be either degenerative or regenerative in nature. Of the seven molecules identified, both beta-arrestin and neurexin 1-beta maintained their altered state at 3 months. Continued down-regulation of Neurexin clearly supports the idea that BBB-related perturbations still persist at 3 months post-treatment, while up-regulation of beta arrestin confirms the continued aberrant signaling pathways mediated by GPCR. Initial up-regulation of Ania-9 at 15 min is followed by significant down-regulation at 3 months, supporting our hypothesis that there is either successful regeneration, or a continuing cell death/atropic state. Continued over-expression of Nos-2a, although slightly decreased at 3 months indicates perturbed nitric oxide metabolism and its possible contribution to cell death mechanisms. Initial down-regulation of PDE at 15 min, followed by up-regulation at 3 months probably indicates recovering cyclic nucleotide metabolism at 3 months from its sarin-induced suppression at 15 min, while continuing severe down-regulation of Gabab-1d at 3 months confirms the hypothesis of defective GABAergic metabolism. Hence early events such as BBB damage (neurein 1-beta), IEGs alteration (Ania-9, probably c-Fos and c-Jun and other Ania members), nitric oxide synthase-mediated pathways (Nos-2a), modified GPCR mediated signaling pathways (mediated by beta arrestin), altered cyclic nucleotide metabolism (PDE2), and inflammation related changes (CX-3C), probably play major role along with other known or unknown mechanisms (as described in Figs. 11 and 12) in sarin-induced pathological changes.

4.13. *Limitations and future directions*

Although the array provides a remarkably comprehensive overview of the gene expression in the CNS after sarin exposure, there are a number of caveats that must be kept in mind. First, the array data provide information on the gene expression at mRNA level only and not on other aspects of gene expression such as protein expression, or post-translational modifications (such as phosphorylation). Even at mRNA level, the information may not be available regarding the mode of transcriptional deregulation, including several mechanisms such as transcriptional activation, repression, and alternate splicing. Nevertheless, one can predict the above-mentioned aspects from global the signature pattern and appropriate modeling as attempted in the current study. These findings will remain speculative until tested individually by other assays. Second, we have examined whole brain gene expression that includes several highly specialized regions such as the cortex, cerebellum, midbrain and

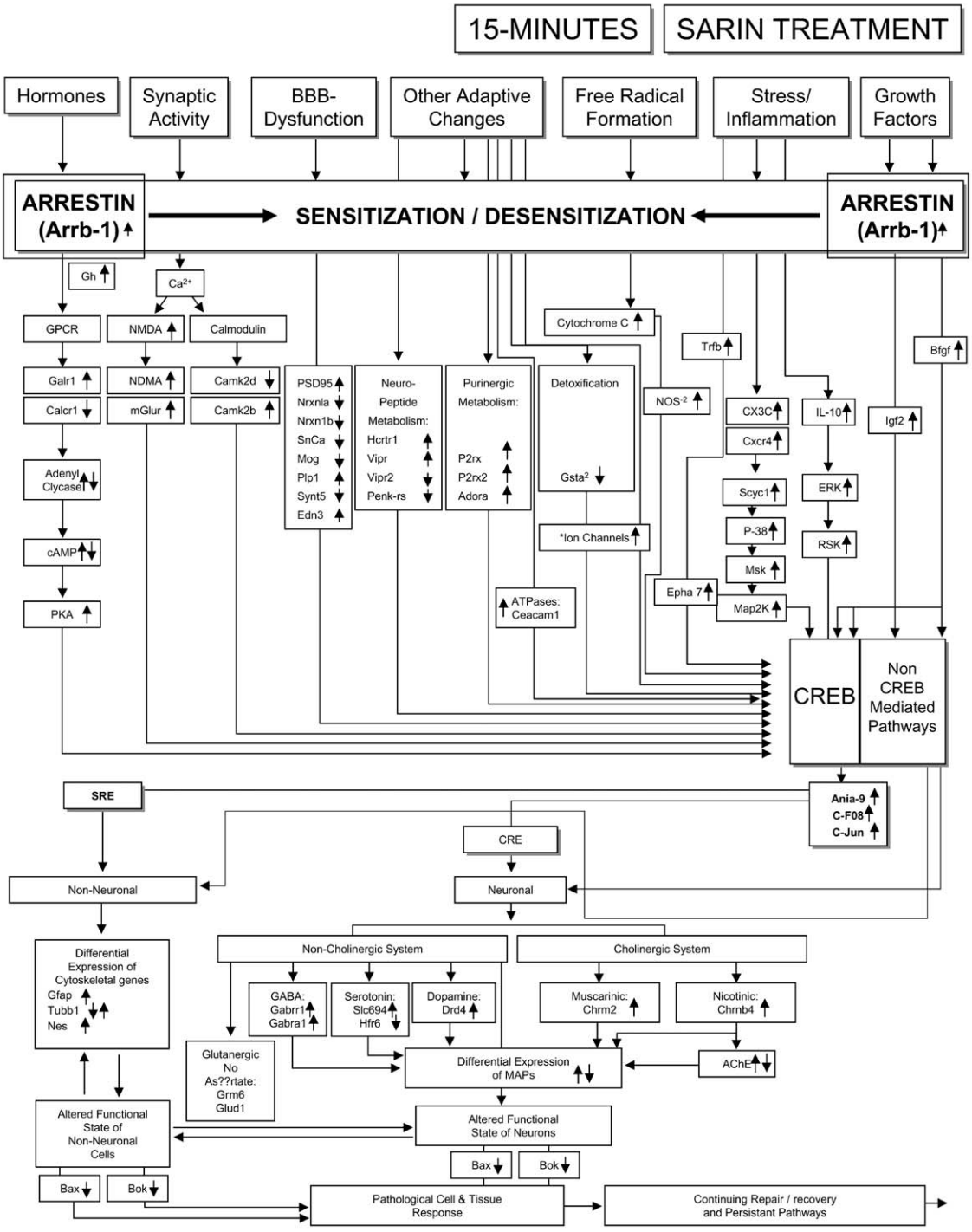

Fig. 11 – Flow chart for the events and the molecules involved in these events at 15-min time point are shown in figure. The pathway figures contain data mostly from the current study along with some data from relevant literature. * Indicates that all of the ion-channel genes were up regulated at 15 min (refer to Table 2) except Kcnn2.

brainstem, which have multitude of specialized cells with specific functions. Although some cell type 'specific' genes can be identified (e.g., endothelial cell-specific genes), most genes on the array are likely to be expressed by many cell types. Third, important changes in a subset of genes could easily be 'diluted' out, markedly lowering the sensitivity of the analysis. Additionally, the large number of genes included in the initial array did not allow for careful analysis of every gene. Although we have undertaken the task of searching all of the relevant literature of several genes, there are many more with significant changes that also merit a literature search in the future. Nevertheless, we already have been able to identify several important processes in sarin-induced neurotoxicity that lead to long-term pathological changes in the rat.

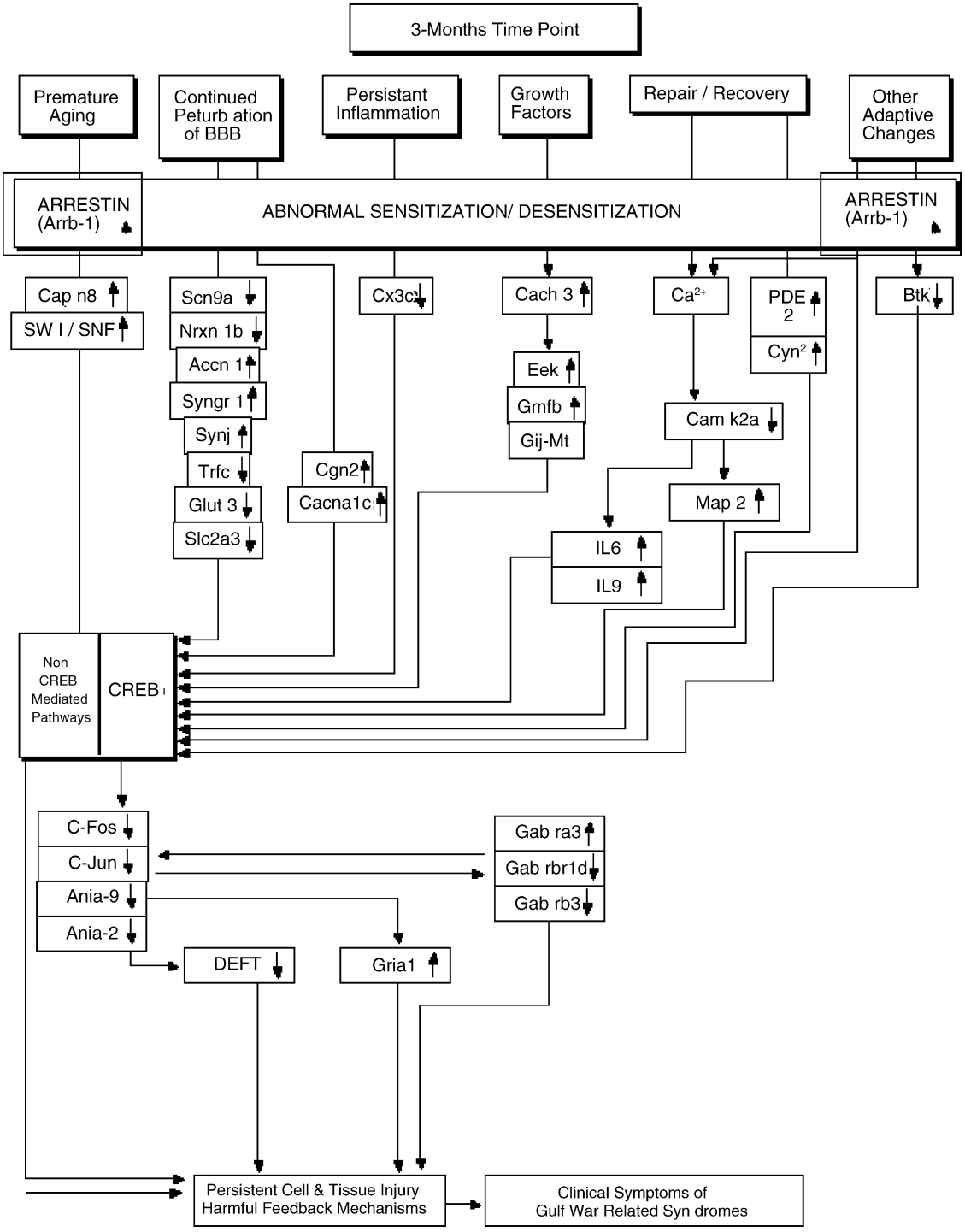

Figs. 12 – This figure depicts the events and molecules involved at 3 months time point. The pathway figures contain data mostly from the current study along with some data from relevant literature.

Acknowledgements

This work is supported in part by the U.S. Army Medical Research and Materiel Command under contract number DAMD 17-98-8027. The views, opinions, and/or findings contained in this report are those of the author(s) and should not be construed as an official Department of the Army positions, policy, or decisions unless so designated by other documentation.

REFERENCES

[1] Afshari CA. Perspective: microarray technology 143(6): 1983–9.
[2] Niijima H, Nagaom I, Nakajima M, Takatori T, Matsuda Y, Iwase H, et al. Sarin-like and soman-like organophosphorous agents activate PLCgamma in rat brains. Toxicol Appl Pharmacol 1999;156(1):64–9.

[3] Taylor P, Brown JH. Acetylcholine. In: Siegel GJ, Agranoff BW, Alberts RW, Fisher SK, Uhler SK, editors. Basic neurochemistry: molecular cellular and medical aspects. New York: Lippincott-Raven; 1999. p. 213–42.
[4] Morita H, Yanagisawa N, Nakajima T, Shimizu M, Hirabayshi H, Okudera M, et al. Sarin poisoning in Matsumuto, Japan. Lancet 1995;14:334–6.
[5] Okumura T, Takasu N, Ishimatsu S, Miyanoki S, Mitsuhashi M, Kumada K, et al. Report on 640 victims of the Tokyo subway sarin attack. Ann Emerg Med 1995;28:129–35.
[6] Yokoyama K, Araki S, Murata K, Nishikitani M, Okumura T, Ishimatsu S, et al. Chronic neurobehavioral effects of Tokyo subway sarin poisoning in relation to posttraumatic stress disorder. Arch Environ Health 1998;53:2489–560.
[7] Smith MI, Elvove E, Frazier WH. The pharmacological action of certain phenol esters with special reference to the etiology of so-called ginger paralysis. Public Health Rep 1930;45:2509–24.
[8] Abou-Donia MB. Organophosphorus ester-induced delayed neurotoxicity. Annu Rev Pharmacol Toxicol 1990;21:511–48.
[9] Himuro K, Murayama S, Nishiyama K, Shinoe T, Iwase H, Nagao M, et al. Distal sensory axonopathy after sarin intoxication. Neurology 1998;51:1195–7.
[10] Davies OR, Holland PR. Effect of oximes and atropine upon the development of delayed neurotoxic signs in chickens following poisoning with DFP and sarin. Biochem Pharmacol 1972;21:3145–51.
[11] Abou-Donia MB. Organophosphorus ester-induced chronic neurotoxicity. Arch Environ Health 2003;58:484–7.
[12] Masuda N, Takatsu M, Morinari H. Sarin poisoning in Tokyo subway. Lancet 1995;345:1446–7.
[13] Sidell, FR. Soman and sarin: clinical manifestations and treatment of accidental poisoning by organophosphates. Clin Toxicol 7:1–17.
[14] Duffy FH, Burchfiel JL, Bartels PH, Goan M, Sim VM. Long-term effects of organophosphate sarin on EEG on monkeys and humans. Neurotoxicology 1:667–89.
[15] Institute of Medicine. Health consequences of service during the Persian Gulf War: Initial findings and recommendations for immediate action. National Academy of Science, Washington, DC, 1995.
[16] Kadar T, Shapira S, Cohen G, Sahar R, Alkalay D, Raveh L. Sarin-induced neuropathology in rats. Hum Exp Toxicol 1995;14(3):252–9.
[17] Abdel-Rahman A, Shetty AK, Abou-Donia MB. Acute exposure to sarin increases blood brain barrier permeability and induces neuropathological changes in the rat: dose-response relationship. Neuroscience 113:721–41.
[18] Damodaran TV, Mecklai AA, Abou-Donia MB. Sarin causes altered time course of mRNA expression of alpha tubulin in the central nervous system of rats. Neurochem Res 2002;27(3):177–81.
[19] Damodaran TV, Bilska MA, Rahman AA, Abou-Doni MB. Sarin causes early differential alteration and persistent overexpression in mRNAs coding for glial fibrillary acidic protein (GFAP) and vimentin genes in the central nervous system of rats. Neurochem Res 2002;27(5):407–15.
[20] Damodaran TV, Jones KH, Patel AG, Abou-Donia MB, Sarin (nerve agent GB)-induced differential expression of mRNA coding for the acetylcholinesterase gene in the rat central nervous system. Biochem Pharmacol 2003;65(12):2041–7.
[21] Dworkin MB, Dawid IB. Use of a cloned library for the study of abundant poly (A) + RNA during Xenopus laevis development. Dev Biol 1980;76:449–64.
[22] Sargentg TD. Isolation of differentially expressed genes. Method Enzymol 1998;152:423–32.
[23] Liang P, Pardee AB. Differential display of eukaryotic messenger RNA by means of the polymerase chain reaction. Science 1992;257(5072):967–71.
[24] Velculescu VE, Zhang L, Vogelstein B, Kinzler KW. Serial analysis of gene expression. Science 1995;270(5235):484–7.
[25] Gupta RP, Abou-Donia MB. Tau phosphorylation by diisopropyl phosphorofluoridate (DFP)-treated hen brain supernatant inhibits its binding with microtubules: role of Ca2+/Calmodulin-dependent protein kinase II in tau phosphorylation. Arch Biochem Biophys 1999;365(2): 268–78.
[26] Gupta RP, Damodaran TV, Abou-Donia MB. C-fos mRNA induction in the central and peripheral nervous systems of diisopropyl phosphorofluoridate (DFP)-treated hens. Neurochem Res 2000;25(3):327–34.
[27] Damodaran TV, Abou-Donia MB. Alterations in levels of mRNAs coding for glial fibrillary acidic protein (GFAP) and vimentin genes in the central nervous system of hens treated with diisopropyl phosphorofluoridate (DFP). Neurochem Res 2000;25(6):809–16.
[28] Damodaran TV, Abdel-Rahman A, Abou-Donia MB. Altered time course of mRNA expression of alpha tubulin in the central nervous system of hens treated with diisopropyl phosphorofluoridate (DFP). Neurochem Res 2001;26(1): 43–50.
[29] Damodaran TV, Abdel-Rahman AA, Suliman HB, Abou-Donia MB. Early differential elevation and persistence of phosphorylated cAMP-response element binding protein (p-CREB) in the central nervous system of hens treated with diisopropyl phosphorofluoridate, an OPIDN-causing compound. Neurochem Res 2002;27(3):183–93.
[30] Larkin JE, Frank BC, Gavras H, Sultana R, Quackenbush J. Independence and reproducibility across microarray platforms. Nat Methods 2005;2(5):337–44.
[31] Hamadeh HK, Bushel PR, Jayadev S, DiSorbo O, Bennett L, Li L, et al. Prediction of compound signature using high density gene expression profiling. Toxicol Sci 2002;67(2):232–40.
[32] Li C, Wong WH. Model-based analysis of oligonucleotide arrays: expression index computation and outlier detection. Proc Natl Acad Sci U S A 2001;98(1):31–6.
[33] Bobashev G, Das S, Das A. A Experimental design for gene microarray experiments and differential expression analysis. In: Johnson K, Lin SM, editors. Methods in microarray analysis II. Boston, MA: Kluwer; 2002.
[34] Siegel GJ, Agranoff BW, Albers RW, Fisher SK, Uhler SK. Basic neurochemistry. Molecular, cellular and medical aspects.. Philadelphia: Lippincott-Raven; 1999.
[35] Gupta RP, Bing G, Hong JS, Abou-Donia MB. cDNA cloning and sequencing of Ca2+/calmodulin-dependent protein kinase IIalpha subunit and its mRNA expression in diisopropyl phosphorofluoridate (DFP)-treated hen central nervous system. Mol Cell Biochem 1998;181(1–2):29–39.
[36] Damodaran T, Patel AG, Abou-Donia MB. Sarin-induced multiple pathways at early time point (2 h) persists at 3 months post treatment; Global expression analysis in a rat model system. Toxicol Sci 2004;78(S-1).
[37] Horikoshi T, Sakakibara M. Quantification of relative mRNA expression in the rat brain using simple RT-PCR and ethidium bromide staining. J Neurosci Methods 2000; 99(1–2):45–51.
[38] Corporation SB, RT 2 End-point Gene Expression Assay Kits. User Manual, part # 1002 version 2.0: 1–10, 2004.
[39] McDonough Jr JH, Shih TM. Neuropharmacological mechanisms of nerve agent-induced seizure and neuropathology. Neurosci Biobehav Rev 1997;21(5): 559–79.
[40] Solberg Y, Belkin M. The role of excitotoxicity in organophosphorous nerve agents central poisoning. Trends Pharmacol Sci 1997;18(6):183–5.
[41] Marrs TC. Organophosphate poisoning. Pharmacol Ther 1993;58(1):51–66.

[42] Ray DE. Chronic effects of low level exposure to anticholinesterrases—a mechanistic review. Toxicol Lett 1998;102–103:527–33.
[43] Cheung NS, Pascoe CJ, Giardina SF, John CA, Beart PM. Micromolar L-glutamate induces extensive apoptosis in an apoptotic-necrotic contiuum of insult-dependent, excitotoxic injury in cultured cortical neurons. Neuropharmacology 1998;37:1419–29.
[44] Sberna G, Saez-Valero J, Li QX, Czech C, Beyreuther K, Masters CL, et al. Acetylcholinesterase is increased in the brains of transgenic mice expressing the C-terminal fragment (CT100) of the ß-amyloid protein precursor of Alzheimer's Disease. J Neurochem 1998;71:723–31.
[45] Calderon FH, von Bernhardi R, De Ferrari G, Luza S, Aldunate R, Inestrosa NC. Toxic effects of acetylcholinesterase on neuronal and glial-like cells in vitro. Mol Psychiatry 1998;3:247–55.
[46] Burchfiel JL, Duffy FH, Van Sim M. Persistent effects of sarin and dieldrin upon the primate electroencephalogram. Toxicol Appl Pharmacol 1976;35(2):365–79.
[47] Woodin AM, Wieneke AA. Action of DFP the leucocyte and the axon. Nature 1970;227(257):460–3.
[48] Pope C, diLorenzo K, Ehrich M. Possible involvement of a neurotrophic factor during the early stages of organophosphate-induced delayed neurotoxicity. Toxicol Lett 1995;75(1–3):111–7.
[49] Smallridge RC, Carr FE, Fein HG. Diisopropylfluorophosphate (DFP) reduces serum prolactin, thyrotropin, luteinizing hormone, and growth hormone and increases adrenocorticotropin and corticosterone in rats: involvement of dopaminergic and somatostatinergic as well as cholinergic pathways. Toxicol Appl Pharmacol 1991;108(2):284–95.
[50] Emoto N, Gonzalez AM, Walicke PA, Wada E, Simmons DM, Shimasaki S, et al. Basic fibroblast growth factor (FGF) in the central nervous system: identification of specific loci of basic FGF expression in the rat brain. Growth Factors 1989;2(1):21–9.
[51] Ozawa K, Uruno T, Miyakawa K, Seo M, Imamura T. Expression of the fibroblast growth factor family and their receptor family genes during mouse brain development. Brain Res Mol Brain Res 1996;41(1–2):279–88.
[52] Datta SR, Dudek H, Tao X, Masters S, Fu H, Gotoh Y, et al. Akt phosphorylation of BAD couples survival signals to the cell-intrinsic death machinery. Cell 1997;91(2):231–41.
[53] Cameron HA, Hazel TG, McKay RD. Regulation of neurogenesis by growth factors and neurotransmitters. J Neurobiol 1998;36(2):287–306.
[54] Agarwal S, Sohal RS. Relationship between aging and susceptibility to protein.
[55] Abu-Qare AW, Abou-Donia MB. Combined exposure to sarin and pyridostigmine bromide increased levels of rat urinary 3-nitrotyrosine and 8-hydroxy-2′-deoxyguanosine, biomarkers of oxidative stress. Toxicol Lett 2001;123: 51–8.
[56] Gupta RC, Milatovic D, Dettbarn WD. Depletion of energy metabolites following acetylcholinesterase inhibitor-induced status epilepticus: protection by antioxidants. Neurotoxicology 2001;22(2):271–82.
[57] Hornsby PJ. Steroid and xenobiotic effects on the adrenal cortex: mediation by oxidative and other mechanisms. Free Radic Biol Med 1989;6(1):103–15.
[58] VanOtteren GM, Standiford TJ, Kunkel SL, Danforth JM, Strieter RM. Alterations of ambient oxygen tension modulate the expression of tumor necrosis factor and macrophage inflammatory protein-1 alpha from murine alveolar macrophages. Am J Respir Cell Mol Biol 1995;13(4):399–409.
[59] DeForge LE, Preston AM, Takeuchi E, Kenney J, Boxer LA, Remick DG. Regulation of interleukin 8 gene expression by oxidant stress. J Biol Chem 1993;268(34):25568–76.
[60] Abou-Donia MB, Dechkovskaia AM, Goldstein LB, Bullman SL, Khan WA. Sensorimotor deficit and cholinergic changes following coexposure with pyridostigmine bromide and sarin in rats. Toxicol Sci 2002;66(1):148–58.
[61] Reynolds IJ, Hastings TG. Glutamate induces the production of reactive oxygen species in cultured forebrain neurons following NMDA receptor activation. J Neurosci 1995;15(5 Pt 1):3318–27.
[62] Haas RH, Nasirian F, Nakano K, Ward D, Pay M, Hill R, et al. Low platelet mitochondrial complex I and complex II/III activity in early untreated Parkinson's disease. Ann Neurol 1995;37(6):714–22.
[63] Joo F. Endothelial cells of the brain and other organ systems: some similarities and differences. Prog Neurobiol 1996;48(3):255–73.
[64] Staddon JM, Smales C, Schulze C, Esch FS, Rubin LL. p120, a p120-related protein (p100), and the cadherin/catenin complex. J Cell Biol 130 1995;(2):369–81.
[65] Black KL. Biochemical opening of the blood-brain barrier. Adv Drug Deliv Rev 1995;15(37).
[66] Mayford M, Kandel ER. Genetic approaches to memory storage. Trends Genet 1999;15(11):463–70.
[67] Kassa J, Koupilova M, Herink J, Vachek J. The long-term influence of low-level sarin exposure on behavioral and neurophysiological functions in rats. Acta Medica (Hradec Kralove) 2001;44(1):21–7.
[68] Kim YM, Barak LS, Caron MG, Benovic JL. Regulation of arrestin-3 phosphorylation by casein kinase II. J Biol Chem 2002;277(19):16837–46.
[69] Wess J. Molecular biology of muscarinic acetylcholine receptors. Crit Rev Neurobiol 1996;10(1):69–99.
[70] Jones KH, Dechkovskaia AM, Herrick EA, Abdel-Rahman AA, Khan WA, Abou-Donia MB. Subchronic effects following a single sarin exposure on blood-brain and blood-testes barrier permeability, acetylcholinesterase, and acetylcholine receptors in the central nervous system of rat: a dose-response study. J Toxicol Environ Health A 2000;61(8):695–707.
[71] Day T, Greenfield SA. A peptide derived from acetylcholinesterase induces neuronal cell death: characterization of possible mechanisms. Exp Brain Res 2003;153:334–42.
[72] Pippig S, Andexinger S, Daniel K, Puzicha M, Caron MG, Lefkowitz RJ, et al. Overexpression of beta-arrestin and beta-adrenergic receptor kinase augment desensitization of beta 2-adrenergic receptors. J Biol Chem 1993;268(5):3201–8.
[73] Oakley RH, Laporte SA, Holt JA, Barak LS, Caron MG. Association of beta-arrestin with G protein-coupled receptors during clathrin-mediated endocytosis dictates the profile of receptor resensitization. J Biol Chem 1999;274(45):32248–57.
[74] Retondaro FC, Doss Santose Costas PC, Pedrosa RC, Kurtenbach E. Presence of antibodies against the third intracellular loop of the M2 muscarinic receptor in the sera of chronic chagasic patients. Faseb J 1999;13(14): 2015–20.
[75] Lee KB, Ptasienski JA, Bunemann M, Hosey MM. Acidic amino acids flanking phosphorylation sites in the M2 muscarinic receptor regulate receptor phosphorylation, internalization, and interaction with arrestins. J Biol Chem 2000;275(46):35767–7.
[76] Niijima H, Nagao M, Nakajima M, Takatori T, Iwasa M, Maeno Y, et al. The effects of sarin-like and soman-like organophosphorus agents on MAPK and JNK in rat brains. Forensic Sci Int 2000;112(2–3):171–8.

[77] Gupta RP, Abdel-Rahman A, Jensen KF, Abou-Donia MB. Altered expression of neurofilament subunits in diisopropyl phosphorofluoridate-treated hen spinal cord and their presence in axonal aggregations.. Brain Res 2000;878(1–2):32–47.
[78] Abou-Donia MB, Goldstein LB, Jones KH, Abdel-Rahman AA, Damodaran TV, Dechkovskaia AM, et al. Locomotor and sensorimotor performance deficit in rats following exposure to pyridostigmine bromide, DEET, and permethrin, alone and in combination. Toxicol Sci 2001;60(2):305–14.
[79] Jariel-Encontre CS, Steff AM, Pariat M, Acquaviva C, Furstoss O, Piechaczyk M. Complex mechanisms for c-fos and c-jun degradation. Mol Biol Rep 1997;24:51–6.
[80] Abou-Donia MB. Involvement of cytoskeletal proteins in the mechanisms of organophosphorus ester-induced delayed neurotoxicity. Clin Exp Pharmacol Physiol 1995;22:358–9.
[81] Baggiolini M. Chemokines and leukocyte traffic. Nature 1998;392(6676):565–8.
[82] Chebib M, Johnston GA. The 'ABC' of GABA receptors: a brief review. Clin Exp Pharmacol Physiol 1999;26(11): 937–40.
[83] Bolin LM, Zhaung A, Strychkarska-Orczyk I, Nelson E, Huang I, Malit M, et al. Differential inflammatory activation of IL-6(−/−) astrocytes. Cytokine 2005;30(2): 47–55.
[84] Barlic J, Khandaker MH, Mahon E, Andrews J, DeVries ME, Mitchell GB, et al. beta-arrestins regulate interleukin-8-induced CXCR1 internalization. J Biol Chem 1999;274(23):16287–94.
[85] Reid S, Ritchie A, Boring L, Gosling J, Cooper S, Hangoc G, et al. Enhanced myeloid progenitor cell cycling and apoptosis in mice lacking the chemokine receptor, CCR2. Blood 1999;93(5):1524–33.
[86] Martin GM. The genetics of aging. Aging (Milano) 1998;10(2):148–9.
[87] Martin GM, Austad SN, Johnson TE. Genetic analysis of ageing: role of oxidative damage and environmental stresses. Nat Genet 1996;13(1):25–34.